# Document

Select the documents you wish to save or order by clicking the box next to the document, or click the link above the document to order directly.



**document 2 of 4** Order Document

**INSPEC - 1969 to date (INZZ)**

**Accession number & update**
6489706, A2000-05-4110H-071, B2000-03-5210-074; 20000201.

**Title**
An efficient algorithm for the RCS modulation prediction from jet inlet-engines.

**Author(s)**
Barka-A; Bobillot-G.

**Author affiliation**
ONERA, Chatillon, France.

**Source**
IEEE Antennas and Propagation Society International Symposium. 1999 Digest, vol.4, Orlando, FL, USA, 11-16 July 1999.
Sponsors: Nat. Sci. Found.
In: p.2566-9 vol.4, 1999.

**ISSN**
ISBN: 0-7803-5639-X, CCCC: 0 7803 5639 X/99/ ($10.00).

**Publication year**
1999.

**Language**
EN.

**Publication type**
CPP Conference Paper.

**Treatment codes**
T Theoretical or Mathematical.

**Abstract**
The electromagnetic scattering from the interior of a complex jet engine inlet contributes significantly to the overall **radar cross section** (RCS) of a modern jet **aircraft.** Previously we have presented a general multi-domain and multi-method coupling scheme, based on generalized scattering matrices computations of three-dimensional inlet subdomains. This method is really suitable in a context of parametric investigations (local inlet engine modifications). In this paper we discuss a new algorithm providing the **radar** modulation due to a set of rotating blades computed with only one solution for any blade position. A validation of this method is presented on a simplified rotating structure connected with an evolutive inlet. (2 refs).

**Descriptors**
aerospace-engines; aircraft; electromagnetic-wave-scattering; finite-element-analysis; integral-equations; modulation; radar-cross-sections; S-matrix-theory.

**Keywords**

efficient algorithm; RCS modulation prediction; jet inlet engines; electromagnetic scattering; **radar cross section;** jet **aircraft;** multi domain coupling scheme; multi method coupling scheme; generalized scattering matrices; three dimensional inlet subdomains; parametric investigations; local inlet engine modifications; algorithm; **radar** modulation; rotating blades; blade position; rotating structure; evolutive inlet; EFIE solver; 3D **finite element** method.

**Classification codes**

A4110H (Electromagnetic waves: theory).
A0260 (Numerical approximation and **analysis**).
B5210 (Electromagnetic wave propagation).
B0290H (Linear algebra (numerical **analysis**)).
B0290T **(Finite element analysis).**
B0290R (Integral equations (numerical **analysis**)).

# Document

Select the documents you wish to save or order by clicking the box next to the document, or click the link above the document to order directly.



☑ **document 1 of 1** Order Document

**INSPEC - 1969 to date (INZZ)**

**Accession number & update**
4484648, A9321-4110H-003, B9311-5210-003; 930916.

**Title**
A new **finite element** formulation for RF scattering by complex bodies of revolution.

**Author(s)**
Khebir-A; D-Angelo-J; Joseph-J.

**Author affiliation**
General Electric Corp Res & Dev, Schenectady, NY, USA.

**Source**
IEEE-Transactions-on-Antennas-and-Propagation (USA), vol.41, no.5, p.534-41, May 1993.

**CODEN**
IETPAK.

**ISSN**
ISSN: 0018-926X, CCCC: 0018-926X/93/ ($03.00).

**Publication year**
1993.

**Language**
EN.

**Publication type**
J Journal Paper.

**Treatment codes**
T Theoretical or Mathematical.

**Abstract**
A formulation for and results of solving electromagnetic scattering from complex inhomogeneous **axisymmetric** bodies are presented. The approach presented uses the **finite element** method in the frequency domain. A node-based approach is used to solve for the three components of the electric or magnetic field. The **finite element** mesh is truncated using a three-dimensional vector absorbing boundary condition based on the Wilcox expansion theorem. A harmonic expansion of the near-field solution obtained from the **finite element** solution is used to compute the far fields and **radar cross section.** (23 refs).

**Descriptors**
boundary-value-problems; electromagnetic-wave-scattering; finite-element-analysis; frequency-domain-analysis; radar-cross-sections.

**Keywords**

electric field; **finite element** formulation; RF scattering; complex bodies of revolution; electromagnetic scattering; inhomogeneous **axisymmetric** bodies; frequency domain; node based approach; magnetic field; **finite element** mesh; three dimensional vector absorbing boundary condition; Wilcox expansion theorem; harmonic expansion; near field solution; far fields; **radar cross section.**

**Classification codes**

A4110H (Electromagnetic waves: theory).
A0260 (Numerical approximation and **analysis**).
B5210 (Electromagnetic wave propagation).
B0290T **(Finite element analysis)**.

# Finite element analysis of axisymmetric radomes

Gordon, R.K. Mittra, R.
Dept. of Electr. Eng., Mississippi Univ., University, MS, USA;

*This paper appears in:* **Antennas and Propagation, IEEE Transactions on**

Publication Date: July 1993
On page(s): 975 - 981
Volume: 41 , Issue: 7
ISSN: 0018-926X
Reference Cited: 9
CODEN: IETPAK
Inspec Accession Number: 4536597

**Abstract:**
A two-step technique for the analysis of axisymmetric radomes is presented. axisymmetric finite-element approach is employed, together with an absorbin condition for mesh truncation, to determine the near fields scattered by an er radome illuminated by a distant source. Next, the reciprocity theorem is invol determine the far-field pattern of an antenna encased by the radome, by com interaction between the current distribution on the antenna and the near-field determined in the first step. The details of the formulation are presented alon numerical results for two different arrays enclosed by radomes of varying per

**Index Terms:**
antenna accessories antenna arrays antenna radiation patterns boundary-value prob element analysis mesh generation absorbing boundary condition axisymmetric rador distribution far-field pattern finite-element approach mesh truncation numerical resu reciprocity theorem scattered near field two-step technique

# Finite Element Analysis of Axisymmetric Radomes

Richard K. Gordon, *Member, IEEE,* and Raj Mittra, *Fellow, IEEE*

***Abstract*—A two-step technique for the analysis of axisymmetric radomes is presented in this paper. Initially, an axisymmetric finite element approach is employed, together with an absorbing boundary condition for mesh truncation, to determine the near fields scattered by an empty radome illuminated by a distant source. Next, the reciprocity theorem is invoked to determine the far-field pattern of an antenna encased by the radome, by computing the reaction between the current distribution on the antenna and the near-field data determined in the first step. The details of the formulation are presented along with numerical results for two different arrays enclosed by radomes of varying permittivities.**

## I. Introduction

THE problem of determining the modification of the radiation pattern of an antenna covered by a radome has been addressed recently by a number of researchers employing a variety of different approaches. Orta *et al.* [1] have used ray optical techniques in conjunction with the reciprocity theorem to address the radome problem, and a geometric theory of diffraction (GTD) approach has been employed by Chikaoka *et al.* [2] to solve the same. Arvas *et al.* [3] have presented a three-dimensional method of moments solution based on the use of the surface equivalence principle, whereas Robinson and his colleagues [4] have used a two-dimensional, oblique-incidence, method-of-moments solution to handle the problem. A two-dimensional finite element analysis that uses an absorbing boundary condition for mesh truncation has been employed by Povinelli and D'Angelo [5], and Chan and Mittra [6] have developed a spectral-domain approach for the analysis of a planar FSS radome.

In this paper, we present a general-purpose method for analyzing axisymmetric radomes with arbitrary inhomogeneities, which cannot be conveniently or accurately investigated by the ray optical techniques, the method of moments, or approximate two-dimensional approaches. We use the reciprocity theorem in conjunction with an axisymmetric finite element approach that employs a novel absorbing boundary condition for mesh truncation. We use a two-step procedure which initially employs the finite element method to determine the near fields within the radome when it is illuminated by a distant source. In the second step, the reciprocity theorem is used to find the far-field pattern of an antenna with a given current distribution located inside the radome, from the near-field information determined earlier in the first step. The method presented here assumes that the presence of the radome does not have a significant effect on the antenna currents; it may not work if these currents are significantly changed by the presence of the radome.

Manuscript received September 25, 1992; revised February 12, 1993.

R. K. Gordon is with the Department of Electrical Engineering, University of Mississippi, University, MS 38677.

R. Mittra is with the Department of Electrical and Computer Engineering, University of Illinois, Urbana, IL 61801.

IEEE Log Number 9211264.

## II. Formulation

The details of the two-step procedure for radome analysis will now be described. To accomplish the first step, which consists of finding the near fields within the radome when it is illuminated by a distant source, we employ a finite element formulation based on the use of scaled versions of the coupled azimuthal potentials (CAP's) [7]. We now present a brief review of the approach used in the first step; for further details, the reader is referred to [8].

We begin by expressing $\boldsymbol{E}$ and $\boldsymbol{H}$ in terms of Fourier series expansions in $\phi$ as

$$\boldsymbol{E}(\rho, \phi, z) = \sum_{m=-\infty}^{\infty} \begin{bmatrix} E_{\rho,m} \\ E_{\phi,m} \\ E_{z,m} \end{bmatrix} e^{jm\phi} \tag{1}$$

$$\boldsymbol{H}(\rho, \phi, z) = \sum_{m=-\infty}^{\infty} \begin{bmatrix} H_{\rho,m} \\ H_{\phi,m} \\ H_{z,m} \end{bmatrix} e^{jm\phi} \tag{2}$$

The potentials we use in this problem are $u_m$ and $v_m$, where

$$u_m = E_{\phi,m} \tag{3}$$

$$v_m = \eta_0 H_{\phi,m}. \tag{4}$$

Inserting (3) and (4) into (1) and (2), and substituting the resulting equations into Maxwell's two curl equations, we obtain six scalar equations for each value of $m$. These six equations can be written as

$$E_{\rho,m} = jf_m\left(m\frac{\partial(\rho u_m)}{\partial\rho} + k_0\rho^2\mu_r\frac{\partial v_m}{\partial z}\right) \tag{5}$$

$$E_{z,m} = jf_m\left(m\rho\frac{\partial u_m}{\partial z} - k_0\rho\mu_r\frac{\partial(\rho v_m)}{\partial\rho}\right) \tag{6}$$

$$H_{\rho,m} = jf_m\left(m\frac{\partial(\rho v_m)}{\partial\rho} - k_0\rho^2\epsilon_r\frac{\partial u_m}{\partial z}\right) \tag{7}$$

$$H_{z,m} = jf_m\left(m\rho\frac{\partial v_m}{\partial z} + k_0\rho\epsilon_r\frac{\partial(\rho u_m)}{\partial\rho}\right) \tag{8}$$

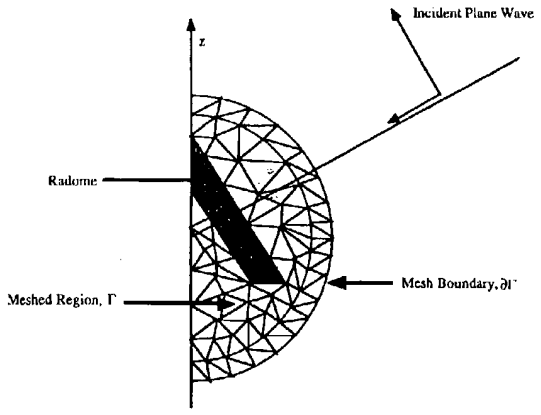


Fig. 1. Finite element mesh for analysis of axisymmetric radome.

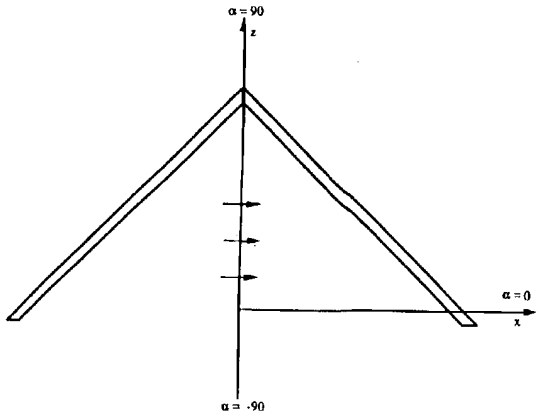


Fig. 3. Vertical array of dipoles.

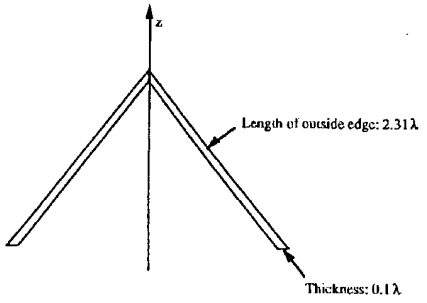


Fig. 2. Radome geometry.

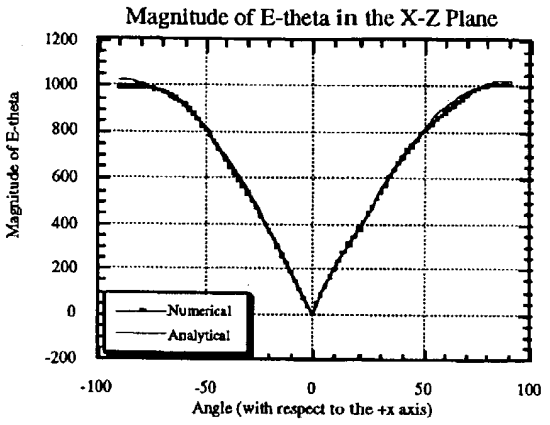


Fig. 4. Comparison of numerically and analytically determined patterns for transparent radome.

$$u_m\epsilon_r+\nabla\cdot(f_m\rho\epsilon_r\nabla(\rho u_m))+(m/k_0)\nabla\cdot(f_m\hat{\phi}\times\nabla(\rho v_m))=0 \tag{9}$$

$$v_m\mu_r+\nabla\cdot(f_m\rho\mu_r\nabla(\rho v_m))-(m/k_0)\nabla\cdot(f_m\hat{\phi}\times\nabla(\rho u_m))=0, \tag{10}$$

where

$$f_m=(k_0^2\mu_r(\rho,z)\epsilon_r(\rho,z)\rho^2-m^2)^{-1}.$$

Equations (3)–(8) demonstrate that $E_{r,m}$, $E_{\phi,m}$, $E_{z,m}$, $H_{r,m}$, $H_{\phi,m}$, and $H_{z,m}$ can be expressed in terms of $u_m$ and $v_m$. This implies that the BOR problem can be solved in terms of just the two unknowns, $u_m$ and $v_m$, rather than all six components of $\boldsymbol{E}$ and $\boldsymbol{H}$. Furthermore, because of the azimuthal symmetry of the body, rather than a three-dimensional mesh, this method requires only a two-dimensional mesh in any $\phi$ = constant plane, such as the one shown in Fig. 1. These two factors result in a significant reduction in the number of unknowns which, in turn, permits the analysis of significantly larger radomes.

Equations (9) and (10) describe the behavior of $u_m$ and $v_m$ in the meshed region. When each of these equations is multiplied by a testing function $T$, and then integrated over the entire meshed region $\Gamma$, the resulting equations can be written, with the help of the divergence theorem, as

$$\begin{aligned}\int\!\!\int_\Gamma Tu_m\epsilon_r\,dA-\int\!\!\int_\Gamma f_m\rho\epsilon_r\nabla T\cdot\nabla(\rho u_m)\,dA\\ -(m/k_0)\int\!\!\int_\Gamma f_m\nabla T\cdot(\hat{\phi}\times\nabla(\rho v_m))\,dA\\ =-\int_{\partial\Gamma}Tf_m\rho\epsilon_r\frac{\partial(\rho u_m)}{\partial n}\,dl-(m/k_0)\\ \cdot\int_{\partial\Gamma}f_mT(\hat{\phi}\times\nabla(\rho v_m))\cdot\hat{n}\,dl\end{aligned} \tag{11}$$

$$\begin{aligned}\int\!\!\int_\Gamma Tv_m\mu_r\,dA-\int\!\!\int_\Gamma f_m\rho\mu_r\nabla T\cdot\nabla(\rho v_m)\,dA\\ +(m/k_0)\int\!\!\int_\Gamma f_m\nabla T\cdot(\hat{\phi}\times\nabla(\rho u_m))\,dA\\ =-\int_{\partial\Gamma}Tf_m\rho\mu_r\frac{\partial(\rho v_m)}{\partial n}\,dl+(m/k_0)\\ \cdot\int_{\partial\Gamma}f_mT(\hat{\phi}\times\nabla(\rho u_m))\cdot\hat{n}\,dl,\end{aligned} \tag{12}$$

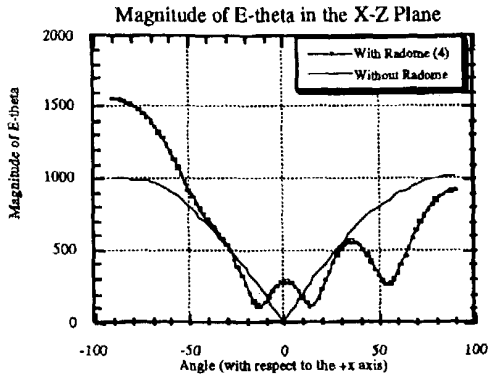


Fig. 5. Effect of radome on antenna pattern for $\epsilon_r$ = (a) 4.0, (b) 8.0, and (c) (4.0, −2.0).

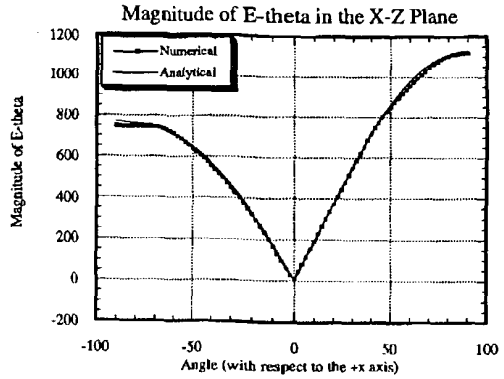


Fig. 6. Comparison of numerically and analytically determined patterns for transparent radome.

where $\partial\Gamma$ is the boundary of the meshed region, $\Gamma$. These are the equations that are implemented using the finite element method. The first term on the right-hand side of each of these equations involves an integral of the normal derivative of an unknown along the outer boundary $\partial\Gamma$. These integrals are evaluated with the assistance of an absorbing boundary condition derived from Wilcox's expansion for the scattered fields [9]. This technique is described in detail in [8].

The finite element solution for the near fields in the vicinity of the radome, when it is illuminated by a plane wave incident at some angle $\theta$ with respect to the $z$ axis, completes the first step of the two-step procedure. Next, the reciprocity theorem is used to find the far field at the desired observation angle, for any antenna located anywhere within the radome. This is the second step of the two-step procedure, and is detailed below.

Let $(\boldsymbol{J}^a, \boldsymbol{M}^a)$ and $(\boldsymbol{J}^b, \boldsymbol{M}^b)$ be two sets of sources existing in the same linear medium and let $\boldsymbol{E}^a$ and $\boldsymbol{H}^a$ be the fields produced by $(\boldsymbol{J}^a, \boldsymbol{M}^a)$ alone, and $\boldsymbol{E}^b$ and $\boldsymbol{H}^b$ be the corresponding fields produced by $(\boldsymbol{J}^b, \boldsymbol{M}^b)$ alone. Then, by invoking the reciprocity theorem, we can show that

$$\int\int\int (\boldsymbol{E}^a \cdot \boldsymbol{J}^b - \boldsymbol{H}^a \cdot \boldsymbol{M}^b)\, d\tau = \int\int\int (\boldsymbol{E}^b \cdot \boldsymbol{J}^a - \boldsymbol{H}^b \cdot \boldsymbol{M}^a)\, d\tau. \tag{13}$$

Thus, for instance, if we set $\boldsymbol{M}^a$ and $\boldsymbol{M}^b$ to be zero, $\boldsymbol{J}^a$ to be the electric current distribution on the antenna, and $\boldsymbol{J}^b$ to be an electric dipole located far from the radome, then (13) can be used to determine the far-zone electric field, $\boldsymbol{E}^a$, of the antenna radiating within the radome. In order to carry out this calculation, both $\boldsymbol{J}^a$ and $\boldsymbol{E}^b$ must be known. We assume that the presence of the radome has little effect on the antenna current distribution; consequently, $\boldsymbol{J}^a$ can be determined through an analysis of the antenna radiating in free space. We also note that $\boldsymbol{E}^b$ is the near electric field in the vicinity of the radome when it is illuminated by the electric dipole $\boldsymbol{J}^b$. But this is precisely what we determined in the first step; that is, the plane wave that is used as the incident field in the first step is chosen to be the field that would be incident upon the radome if it were radiated by $\boldsymbol{J}^b$. Thus, the electric field determined in the first step is identical to $\boldsymbol{E}^b$. So, once the first step has been concluded for a particular location of $\boldsymbol{J}^b$, (13) can be used to find, at this same location, the electric field radiated by the antenna within the radome. Similarly, the far magnetic field can be determined by setting $\boldsymbol{J}^b$ equal to

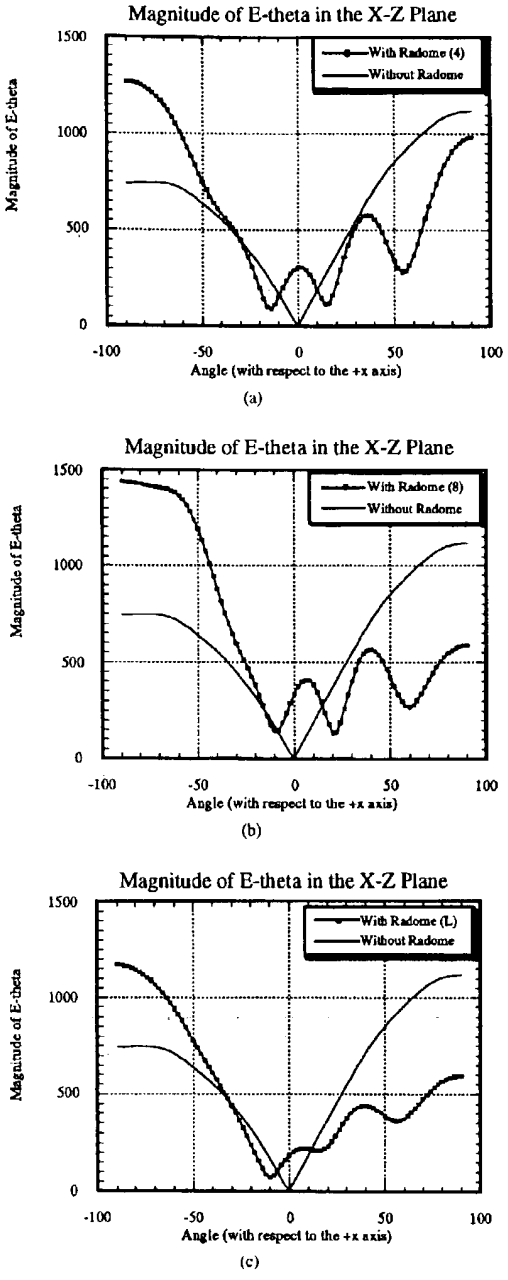


Fig. 7. Effect of radome on antenna pattern for $\epsilon_r$ = (a) 4.0, (b) 8.0, and (c) (4.0, −2.0).

zero and letting $\boldsymbol{M}^b$ be a magnetic dipole located far from the radome. We note at this point that it is unnecessary to recalculate the finite element matrix for each new location of $\boldsymbol{J}^b$ or $\boldsymbol{M}^b$; these sources affect only the incident field. Thus, the amount of computer time required to solve for 90 different source locations is only twice that required for a

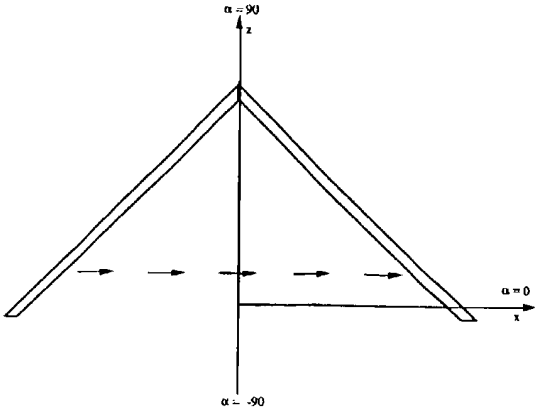


Fig. 8. Horizontal array of dipoles.

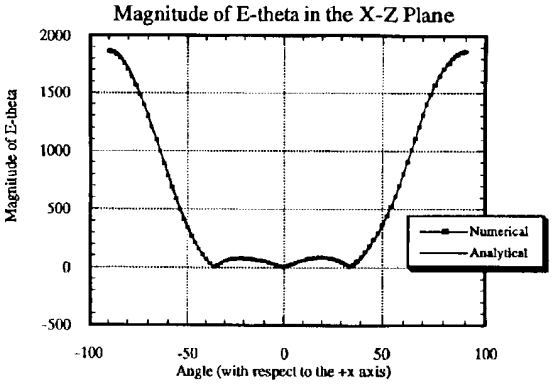


Fig. 9. Comparison of numerically and analytically determined patterns for transparent radome.

single location. Furthermore, we note that while the radome must have azimuthal symmetry, the antenna may have any shape and may be located anywhere within the radome. We now consider some numerical examples to demonstrate the use of this method.

## III. Numerical Results

In this section we present some numerical results that illustrate the use of the method described above to analyze the radome geometry shown in Fig. 2. In each case, we consider a radome that has the shape of a truncated cone which is open at the bottom, although the method itself is general enough to handle any kind of closure of the radome, as long as the azimuthal symmetry is maintained. The length of the outside edge of the cone is $2.31\lambda_0$; its thickness is $0.1\lambda_0$. We will present the effects of varying the relative permittivity of the radome on the radiation patterns of two antenna arrays.

The first case we consider is shown in Fig. 3. The antenna is an array of three uniformly excited $x$-directed dipoles located on the $z$ axis. The distance between consecutive dipoles is $0.0854\lambda_0$. We use the two-step procedure described above

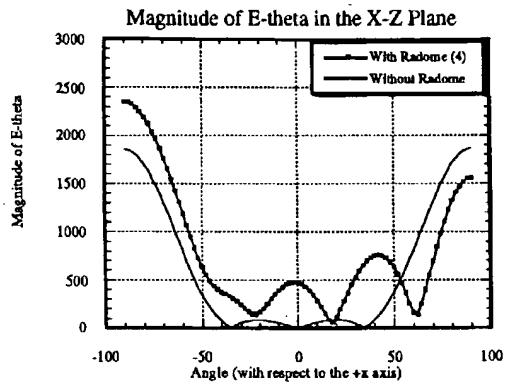


Fig. 10. Effect of radome on antenna pattern for $\epsilon_r$ = (a) 4.0, (b) 8.0, and (c) (4.0, −2.0).

to determine the far-field value of $E_\theta$ in the plane $\phi = 0°$ for four different radome permittivities: $\epsilon_r = 1.0$, 4.0, 8.0, and (4.0, −2.0). The results for $\epsilon_r = 1.0$ are shown in Fig. 4. The reason we consider the case $\epsilon_r = 1.0$, i.e., the case of a transparent radome, is that for this problem an analytically determined pattern can be obtained for comparison

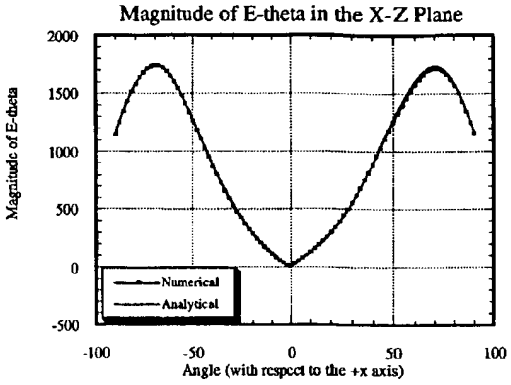


Fig. 11. Comparison of numerically and analytically determined patterns for transparent radome.

with the numerical results. As we can see from Fig. 4, in which the dotted line represents the numerical results while the solid line depicts the analytically determined pattern, the comparison is quite favorable. Note that this does not prove the validity of this technique but is a good check. In Fig. 5, we show the numerical results for $\epsilon_r$ = (a) 4.0, (b) 8.0, and (c) (4.0, −2.0). In each case, the dotted line represents the radiation pattern in the presence of the radome while the solid line depicts the pattern obtained in its absence. We note that, in each case, the null at 0°, i.e., in the positive $x$ direction, has disappeared. The enhancement of the pattern near −90° can be attributed to the fact that the radome is open at the bottom. We also note the degradation of the pattern for most positive angles, i.e., looking through the radome.

In Figs. 6 and 7 we consider the same vertical array of three dipoles; but while the amplitude of the excitation for each dipole is still the same, a phase progression has now been introduced. The phase of the excitation on the bottom, middle, and top dipole, is 0.0°, −27.86°, and −55.72°, respectively. Fig. 6 presents a comparison of the numerical and analytically determined results for the transparent radome, while Fig. 7 shows the effect on the radiation pattern of the presence of a radome of relative permittivity (a) 4.0, (b) 8.0, and (c) (4.0, −2.0). Like Fig. 4 above, Fig. 6 shows good agreement between the numerical results and the analytically determined pattern for the transparent radome. Fig. 7 shows the same general features that were observed in Fig. 5, but in this case the phase progression is present.

The second case we consider is shown in Fig. 8. The antenna is a horizontal array of five uniformly excited $x$-directed dipoles. The distance between consecutive dipoles is $0.247\lambda_0$. We again use the two-step procedure to determine the far-field value of $E_\theta$ in the plane $\phi = 0°$ for four different radome permittivities: $\epsilon_r = 1.0$, 4.0, 8.0, and (4.0, −2.0). The results for $\epsilon_r = 1.0$ are shown in Fig. 9. Just as was the case for the vertical array, we see that there is good agreement between the numerical results and the analytically determined pattern for this horizontal array of uniformly excited dipoles. In Fig. 10 we see the numerical results for $\epsilon_r$ = (a) 4.0, (b) 8.0, and (c) (4.0, −2.0). We again note that as a result of the introduction

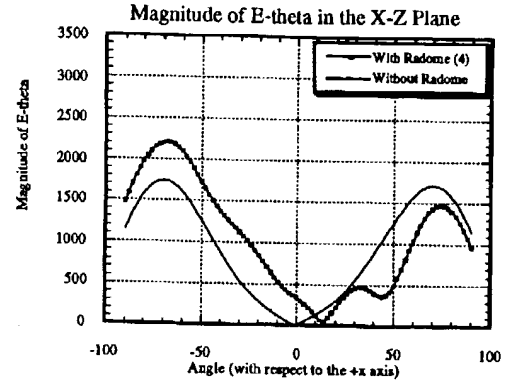


Fig. 12. Effect of radome on antenna pattern for $\epsilon_r$ = (a) 4.0, (b) 8.0, and (c) (4.0, −2.0).

of the radome, the null at 0° has disappeared, the pattern has been enhanced near −90°, and the pattern has been diminished at angles near +90°.

The final results we present are for the same horizontal array of dipoles when the amplitude of the excitations is uniform but a phase progression is used. Proceeding from left to right, the phases of the excitation on the first, second, third, fourth, and fifth dipoles are −75.16°, −37.58°, 0.0°, 37.58°, and 75.16°, respectively. Fig. 11 presents a comparison of the numerical and analytically determined results for the transparent radome, while Fig. 12 shows the effect on the radiation pattern of the presence of a radome of relative permittivity (a) 4.0, (b) 8.0, and (c) (4.0, −2.0). We again note, in Fig. 11, the good agreement between the numerical results and the analytically determined pattern for the transparent radome. Fig. 12 shows the expected effects of the presence of the radome on the antenna pattern.

## IV. Conclusions

In this paper, we have considered a two-step technique for the analysis of inhomogeneous axisymmetric radomes. We have verified the approach by computing the radiation pattern of an unphased vertical array of dipoles, a phased vertical array of dipoles, an unphased horizontal array of dipoles, and a phased horizontal array of dipoles within a transparent radome for which the radiation pattern can be determined analytically. Next, we investigated the pattern of these same antennas covered by two lossless radomes and one lossy radome. By comparing the results for each case, it is possible to determine how the radiation pattern is affected by a change in the composition of the radome. Similarly, this method could also be used to determine the effect of changing the shape of the radome or the addition of a metallic tip.

## Acknowledgment

The authors would like to thank the National Center for Supercomputing Research at the University of Illinois and the Mississippi Center for Supercomputing Research at the University of Mississippi for the help they provided in generating the numerical results presented in this paper.

## References

[1] R. Orta, R. Tascone, and R. Zich, "Performance degradation of dielectric radome covered antennas," *IEEE Trans. Antennas Propagat.*, vol. 36, pp. 1707–1713, Dec. 1988.

[2] S. Chikaoka, I. Chiba, Y. Sunahara, T. Numazaki, and S. Mano, "Pattern synthesis of an array antenna in a radome," *Dig. 1990 IEEE Antennas Propagat. Soc. Int. Symp.*, vol. 2, May 1990, pp. 1852–1855.

[3] E. Arvas, A. Rahhalarabi, U. Pekel, and E. Gundogan, "Electromagnetic transmission through a small radome of arbitrary shape," *Proc. Inst. Elec. Eng.*, vol. 137, pt. H, no. 6, Dec. 1990.

[4] A. J. Robinson, B. Chambers, and J. C. Bennett, "Electromagnetic modelling of impedance-loaded dielectric space-frame radomes," in *Proc. Seventh Int. Conf. Antennas Propagat., ICAP 91*, vol. 1, Apr. 1991, pp. 460–463.

[5] M. J. Povinelli and J. D'Angelo, "Finite element analysis of large wavelength antenna radome problems for leading edge and radar phased arrays," *IEEE Trans. Magn.*, vol. 27, pp. 4299–4302, Sept. 1991.

[6] C. Chan and R. Mittra, "Investigation of antenna interaction with an FSS radome," in *Dig. 1989 IEEE Antennas Propagat. Soc. Int. Symp.*, vol. 2, June 1989, pp. 1076–1079.

[7] M. A. Morgan, S. K. Chang, and K. K. Mei, "Coupled azimuthal potentials for EM field problems in inhomogeneous axially symmetric media," *IEEE Trans. Antennas Propagat.*, vol. 25, pp. 413–417, May 1977.

[8] R. K. Gordon and R. Mittra, "PDE techniques for solving the problem of radar scattering by a body of revolution," *Proc. IEEE*, vol. 79, pp. 1449–1458, Oct. 1991.

[9] C. H. Wilcox, "An expansion theorem for electromagnetic fields," *Commun. Pure Appl. Math.*, vol. IX, pp. 115–134, 1956.

**Richard K. Gordon** (S'89–M'90) was born in Birmingham, AL, on November 26, 1959. He received the B.S. degree in physics from Birmingham-Southern College in 1983 and the M.S. degree in applied mathematics and the Ph.D. degree in electrical engineering from the University of Illinois at Urbana-Champaign in 1986 and 1990, respectively.

From May 1987 to August 1990 he worked as a research assistant in the Electromagnetic Communications Laboratory at the University of Illinois. In August 1990 he was appointed Assistant Professor in the Department of Electrical Engineering at the University of Mississippi. His research interests include the use of partial differential approaches for the solution of open-region and closed-region problems in electromagnetics, numerical techniques, and the mathematical methods of electromagnetics.

Dr. Gordon is a member of Phi Kappa Phi, Phi Beta Kappa, and Eta Kappa Nu.

**Raj Mittra** (S'54–M'57–SM'69–F'71) is the Director of the Electromagnetic Communication Laboratory of the Electrical and Computer Engineering Department and Research Professor of the Coordinated Science Laboratory at the University of Illinois. He is a Past-President of AP-S, and he has served as the editor of the Society's TRANSACTIONS ON ANTENNAS AND PROPAGATION. He won the Guggenheim Fellowship Award in 1965 and the IEEE Centennial Medal in 1984. He has been a Visiting Professor at Oxford University, Oxford, England and at the Technical University of Denmark, Lyngby, Denmark. Currently, he serves as the North American editor of the journal *AEÜ*. He is President of RM Associates, a consulting organization providing services to several industrial and governmental organizations.

His professional interests include the areas of computational electromagnetics, electromagnetic modeling of electronic packaging, radar scattering, satellite antennas, microwave and millimeter-wave integrated circuits, frequency selective surfaces, and EMP and EMC analysis.

Dr. Mittra has published over 350 journal papers and 20 books or book chapters on various topics related to electromagnetics.

# Coupled azimuthal potentials for electromagnetic fi problems in inhomogeneous axially symmetric med

Morgan, M. Shu-Kong Chang Mei, K.
University of California, Berkeley, Berkeley, CA, USA

*This paper appears in:* **Antennas and Propagation, IEEE Transactions on pre - 1988]**

Publication Date: May 1977
On page(s): 413 - 417
Volume: 25 , Issue: 3
ISSN: 0096-1973

**Abstract:**
Classical electromagnetic potential formulations are, with the exceptions of a cases of one-dimensional stratification, restricted to use in uniform media. A developed potential formulation that provides a flexible basis for numerical co of time-harmonic field problems involving continuously and discretely inhomo axially symmetric media is the topic of this paper. The formulation manifests both a differential equation system and, alternately, a variational criterion. Ty numerical applications include solutions of scattering by arbitrarily shaped ma bodies of revolution and radiation from inhomogeneously loaded rotationally s antenna structures. Current numerical investigations by the authors, using M unimoment method in conjunction with both finite-difference and finite-eleme techniques, have shown the formulation to be highly feasible for computation problems having dimensions as large as several wavelengths.

**Index Terms:**
Electromagnetic scattering by nonhomogeneous media Loaded antennas Nonhomoge media Numerical methods

Publications | Help | FAQ| Terms | Back to Top

[6] M. I. Kontorovich, V. Yu. Petrun'kin, N. A. Yesepkina, and M. I. Astrakhan, "The coefficient of reflection of a plane electromagneitc wave from a plane wire mesh," *Radio Engr. and Elect. Phys.*, vol. 7, pp. 221–331, Feb. 1962.
[7] N. M. Zolotukhina, "Averaged boundary conditions for a two-dimensional slot array," *Radio Engr. Elect. Phys.*, vol. 20, pp. 112–114, Mar. 1975.
[8] G. J. van den Broek and J. van der Vooren, "Reflection properties of periodically supported metallic wire gratings with rectangular mesh showing small sag," *IEEE Trans. Antennas Propagat.*, vol. AP-19, pp. 109–113, Jan. 1971.

## Coupled Azimuthal Potentials for Electromagnetic Field Problems in Inhomogeneous Axially Symmetric Media

MICHAEL A. MORGAN, STUDENT MEMBER, IEEE,
SHU-KONG CHANG, STUDENT MEMBER, IEEE,
AND KENNETH K. MEI, MEMBER, IEEE

*Abstract*—Classical electromagnetic potential formulations are, with the exceptions of a few special cases of one-dimensional stratification, restricted to use in uniform media. A recently developed potential formulation that provides a flexible basis for numerical computation of time-harmonic field problems involving continuously and discretely inhomogeneous axially symmetric media is the topic of this paper. The formulation manifests itself in both a differential equation system and, alternately, a variational criterion. Typical numerical applications include solutions of scattering by arbitrarily shaped material bodies of revolution and radiation from inhomogeneously loaded rotationally symmetric antenna structures. Current numerical investigations by the authors, using Mei's unimoment method in conjunction with both finite-difference and finite-element techniques, have shown the formulation to be highly feasible for computation of field problems having dimensions as large as several wavelengths.

### I. INTRODUCTION

Numerical computation of time-harmonic electromagnetic boundary value problems has recently been extended into the regime of inhomogeneous axially symmetric media by way of the potential formulation to be presented in this paper. This formulation provides the basis for the numerical solution of an important class of interior, radiation, and scattering problems, involving inhomogeneous bodies of revolution having multiwavelength dimensions, which were heretofore unapproachable using conventional techniques.

Electromagnetic fields are traditionally represented in terms of potentials for ease of analysis. Potential formulations also offer numerical advantages by usually having fewer coupled unknowns and a higher order of continuity than the original electromagnetic field. Computation time is, in fact, proportional to the cube of the number of coupled scalar fields which are present as unknowns in the formulation. A general vector potential representation may be developed for completely arbitrary inhomogeneous isotropic material, but the formulation is in terms of four coupled scalar fields [1]. Without potentials, Maxwell's equations must be solved using at least three coupled scalar functions: namely the vector of either the electric or the magnetic field, which are in general discontinuous at material interfaces. Classical TE and TM potential formulations generate all fields from only two uncoupled scalar functions, but are only valid for uniform media and some special cases of separable coordinate one-dimensional inhomogeneities, such as that of a spherically stratified media [1], [2].

Manuscript received February 23, 1976. This work was sponsored by U.S. Army Mobility Equipment Research and Development Center Contract DAAK02-75-C-002.

The authors are with the Department of Electrical Engineering and Computer Sciences and the Electronics Research Laboratory, University of California, Berkeley, CA 94720.

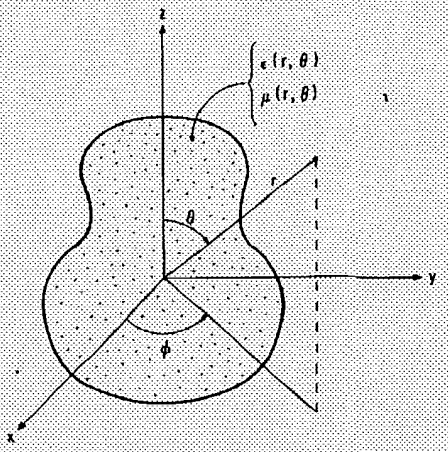


Fig. 1. Axially symmetric inhomogeneous medium.

The potential formulation to be presented here is valid in generally inhomogeneous isotropic rotationally symmetric media, as shown in Fig. 1, where the constitutive parameters $\epsilon(\bar{r})$ and $\mu(\bar{r})$ are invariant to the azimuthal coordinate $\phi$. All electromagnetic field components are expanded via exponential Fourier series in the $\phi$-coordinate. The modal electromagnetic fields are shown to be representable by two coupled azimuthal potentials (CAP's), so named because of their one-to-one relationship with the azimuthal components of the modal electric and magnetic fields. The potentials in the CAP formulation, which are everywhere continuous, are then shown to satisfy a system of coupled partial differential equations and, alternately, a variational criterion, either of which can be used as a basis for developing numerical solution algorithms.

The range of possible application of this new potential representation of Maxwell's equations includes the numerical solutions of both interior region Dirichlet type problems and open region radiation and scattering problems, using Mei's "unimoment method" [3]. The CAP formulation can be readily employed, in conjunction with appropriate numerical techniques, to solve such typical problems as scattering by distorted raindrops, power absorption by azimuthally invariant biological tissue models, and effects of inhomogeneous dielectric loading on axially symmetric antenna structures and waveguide sections.

### II. MODAL FIELD DECOMPOSITION AND GENERATING EQUATIONS

The normalized coordinates to be used in the subsequent equations are defined by $(R, Z, \phi) = (k_0\rho, k_0 z, \phi)$, where $(\rho, z, \phi)$ are standard circular cylindrical coordinates and $k_0 = 2\pi/\lambda_0$ is the free-space wavenumber of the time-harmonic

field. The reason for this particular choice of coordinates is twofold. First, the use of this normalized coordinate system yields very compact equation presentations, and second, these coordinates form a two-dimensional Cartesian system in the spatial solution domain for the CAP formulation. This latter property is of particular value for use with the finite-element method, where numerical surface integrations must be performed over the two-dimensional spatial solution domain. The relative constitutive parameters of the medium, $\epsilon_r(R, Z)$ and $\mu_r(R, Z)$, are invariant to the $\phi$-coordinate.

The equations of the CAP formulation are obtained by first decomposing the total fields into azimuthal modes via an exponential Fourier series in the $\phi$-coordinate

$$\bar{E}(R, Z, \phi) = \sum_{m=-\infty}^{\infty} \bar{e}_m(R, Z) \exp(jm\phi) \tag{1a}$$

$$\eta_0 \bar{H}(R, Z, \phi) = \sum_{m=-\infty}^{\infty} \bar{h}_m(R, Z) \exp(jm\phi) \tag{1b}$$

where $\eta_0 = 120\pi\ \Omega$. Due to the assumed axial symmetry of the medium, the modal fields have time-average power orthogonality and decouple when the field expansions in (1) are substituted into Maxwell's time-harmonic source-free equations, yielding the first-order coupled system given by

$$\epsilon_r e_{\phi,m} = j\left[\frac{\partial h_{Z,m}}{\partial R} - \frac{\partial h_{R,m}}{\partial Z}\right] \tag{2a}$$

$$\mu_r h_{\phi,m} = j\left[\frac{\partial e_{R,m}}{\partial Z} - \frac{\partial e_{Z,m}}{\partial R}\right] \tag{2b}$$

$$R\epsilon_r e_{R,m} = j\left[\frac{\partial (R h_{\phi,m})}{\partial Z} - jm h_{Z,m}\right] \tag{2c}$$

$$R\mu_r h_{R,m} = j\left[jm e_{Z,m} - \frac{\partial (R e_{\phi,m})}{\partial\ \partial Z}\right] \tag{2d}$$

$$R\epsilon_r e_{Z,m} = j\left[jm h_{R,m} - \frac{\partial (R h_{\phi,m})}{\partial R}\right] \tag{2e}$$

$$R\mu_r h_{Z,m} = j\left[\frac{\partial (R e_{\phi,m})}{\partial R} - jm e_{R,m}\right] \tag{2f}$$

where the azimuthal dependence of the modal fields is suppressed. Using judicious substitution between (2c) and (2f), and between (2d) and (2e), it is easily found that all modal field components can be generated from two modal scalar potential functions $\psi_1(R, Z, m)$ and $\psi_2(R, Z, m)$, via

$$\hat{\phi} \times \bar{e}_m = j f_m (m\hat{\phi} \times \nabla\psi_1 - R\mu_r \nabla\psi_2) \tag{3a}$$

$$\hat{\phi} \cdot \bar{e}_m = \psi_1 / R \tag{3b}$$

$$\hat{\phi} \times \bar{h}_m = j f_m (m\hat{\phi} \times \nabla\psi_2 + R\epsilon_r \nabla\psi_1) \tag{3c}$$

$$\hat{\phi} \cdot \bar{h}_m = \psi_2 / R \tag{3d}$$

where $\hat{\phi}$ is the unit azimuthal vector, the two-dimensional gradient operator is defined by

$$\nabla = \hat{R}\frac{\partial}{\partial R} + \hat{Z}\frac{\partial}{\partial Z} \tag{4a}$$

and

$$f_m(R, Z) = [\mu_r(R, Z)\epsilon_r(R, Z)R^2 - m^2]^{-1}. \tag{4b}$$

As was previously mentioned, the normalized cylindrical coordinates $(R, Z, \phi)$ were chosen only for the practical reasons of compact presentation and utility in finite-element numerical computations. The equations of the CAP formulation can be easily obtained in an arbitrary coordinate system $(u_1, u_2, \phi)$, where $u_1$ and $u_2$ are both orthogonal to $\phi$ and form some single-valued system of coordinates in any constant azimuth planar cross section of the region of revolution. For example, the equations throughout this paper can be trivially recast into standard spherical coordinates $(r, \theta, \phi)$ using the simple substitutions $R = k_0 r \sin\theta$, $Z = k_0 r \cos\theta$, and $\nabla = [(1/k_0)\hat{r}(\partial/\partial r) + \hat{\theta}(1/r)(\partial/\partial\theta)]$.

A very important property of the potentials can be obtained easily by noting that since the modal potentials are proportional to the $\phi$-components of $\bar{e}_m$ and $\bar{h}_m$, as shown in (3b) and (3d), they are continuous everywhere, including at dielectric and magnetic interfaces. This property of uniform field continuity is very desirable in numerical computations. For the case of the variational finite-element method the utility of the potential field continuity is particularly pronounced, in that material interfaces require no supplemental boundary conditions and are handled naturally with the same general algorithm as is continuously inhomogeneous media.

## III. DIFFERENTIAL EQUATION REPRESENTATION

The partial differential equations obeyed by the coupled azimuthal potentials $\psi_1$ and $\psi_2$ may be obtained directly from Maxwell's equations by substitution of the modal field generating equations in (3) into (2a) and (2b). The potentials are found to satisfy a system of coupled second-order linear partial differential equations given by

$$\nabla \cdot [f_m(R\epsilon_r \nabla\psi_1 + m\hat{\phi} \times \nabla\psi_2)] + \epsilon_r \psi_1 / R = 0 \tag{5a}$$

$$\nabla \cdot [f_m(R\mu_r \nabla\psi_2 - m\hat{\phi} \times \nabla\psi_1)] + \mu_r \psi_2 / R = 0 \tag{5b}$$

where the gradient operator $\nabla$ is as defined previously in (4a) and $f_m(R, Z)$ is given by (4b).

To utilize the unimoment technique in obtaining solutions to open region radiation and scattering problems requires the ability to solve interior Dirichlet type boundary value problems within a closed region containing the inhomogeneities of the problem, (e.g., an antenna structure or scattering bodies). In solving such an interior Dirichlet problem the two-dimensional solution domain of (5) is a planar constant-$\phi$ cross section of an interior volume of revolution, as is illustrated in Fig. 2. The interior region $S$, which is bounded by the curve $C$, contains inhomogeneous material specified by the relative constitutive parameters $\epsilon_r(R, Z)$ and $\mu_r(R, Z)$. The surface $S$ could, for example, be the semicircular cross section of a geometrical sphere which contains an arbitrarily shaped, (and possibly inhomogeneous), material body of revolution, such as a torus.

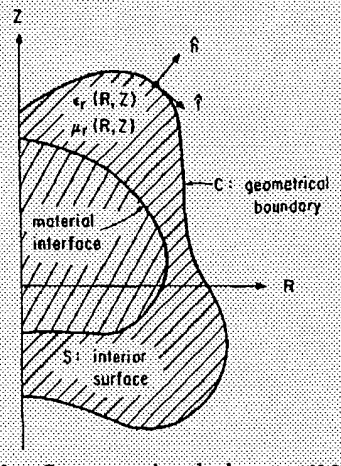


Fig. 2. Constant azimuth planar cross section.

The question of uniqueness of the solution to the coupled system in (5), for arbitrary Dirichlet boundary conditions of the potentials specified on $C$, may be resolved by using the standard proof for electromagnetic field uniqueness assuming nonzero losses [4], where it is noted that $\psi_1$ and $\psi_2$ are proportional to the $\phi$-components of $\bar{e}_m$ and $\bar{h}_m$, respectively.

For the special case of azimuthally invariant modal fields ($m = 0$), the differential equations in (5) decouple, giving a simple potential formulation that was originally derived by Abraham and is given more currently by Stratton [5]. This uncoupled formulation was the basis for a recently completed investigation of inhomogeneous dielectric loading of biconical antenna structures, conducted by Stovall and Mei, using finite-difference simulation of the PDE for $\psi_2$ when $m = 0$ [6]. It should be noted that only for the case of the axially symmetric mode ($m = 0$), can the total modal field be decomposed into partial fields which are either TE or TM to $\hat{\phi}$. This constraint expresses the fact that no azimuthally changing modal electromagnetic field ($m \neq 0$) can be generated having a null azimuthal component of either $\bar{e}_m$ or $\bar{h}_m$ throughout an axially symmetric source-free volume of revolution. This result is valid even when $\epsilon$ and $\mu$ are constant, which is perhaps the reason why the CAP formulation has been overlooked by classical electromagnetic analysts.

To further investigate the nature of the system of CAP PDE's in (5) we will use matrix operator notation to recast the equations into a more compact form. Defining the solution vector

$$\psi(R, Z, m) = \begin{bmatrix} \psi_1(R, Z, m) \\ \psi_2(R, Z, m) \end{bmatrix} \tag{6}$$

and the matrix differential operator

$$\mathsf{A}(R, Z, m) = \begin{bmatrix} \nabla \cdot (f_m R \epsilon_r \nabla) + \epsilon_r / R & m \nabla \cdot (f_m \hat{\phi} \times \nabla) \\ -m \nabla \cdot (f_m \hat{\phi} \times \nabla) & \nabla \cdot (f_m R \mu_r \nabla) + \mu_r / R \end{bmatrix} \tag{7}$$

the system in (5) is given by

$$\mathsf{A}\psi = \mathbf{0} \tag{8a}$$

with Dirichlet BC's on $C$ given by

$$\psi(R, Z, m)\,|_C = \beta(c). \tag{8b}$$

A very important property of the operator $\mathsf{A}$ is its formal self-adjointness on the space of vector functions having homogeneous Dirichlet BC's on $C$,

$$\langle u, \mathsf{A}v \rangle = \langle v, \mathsf{A}u \rangle \tag{9}$$

where the nonconjugated inner dot product is defined by

$$\langle a, b \rangle = \int_S a(R, Z) \cdot b(R, Z)\, dR\, dZ \tag{10}$$

and the vector functions in (9) satisfy the adjoint boundary condition $u\,|_C = v\,|_C = 0$. As a consequence of this operator self-adjointness it follows directly that a variational principle exists for the CAP formulation.

## IV. VARIATIONAL FORMULATION

The numerical solution of the system of PDE's in (5) via finite-difference simulation requires the use of basis functions which are twice differentiable. This continuity constraint on the basis functions may be relaxed to only first-order differentiability if a variational formulation is used in conjunction with the finite-element method.

In establishing a variational principle we will follow two separate, but equivalent, routes. Our first avenue is the Euler–Lagrange formulation which provides the simplest, but somewhat indirect, approach to a variational criterion. The second development relies upon the self-adjointness of the system operator $\mathsf{A}$ in conjunction with the application of a stationary theorem, to provide direct access to a variational principle.

The Euler–Lagrange variational formulation is based upon the existence of a functional of the potentials and their first derivatives which is stationary about the correct solution of (5) for given Dirichlet BC's on the boundary curve $C$ of Fig. 2. The functional manifests itself as a surface integral over the planar cross section surface $S$,

$$F = \int_S L(R, Z, \psi_1, \psi_2, \nabla\psi_1, \nabla\psi_2)\, dR\, dZ \tag{11}$$

It is well known from the calculus of variations that at the stationary point of the functional $F$ the Lagrangian $L$ satisfies a system of coupled Euler–Lagrange partial differential equations [7],

$$\nabla \cdot \left[ \frac{\partial L}{\partial(D_R \psi_k)} \hat{R} + \frac{\partial L}{\partial(D_Z \psi_k)} \hat{Z} \right] - \frac{\partial L}{\partial \psi_k} = 0, \quad k = 1, 2. \tag{12}$$

The foremost problem in deriving such a variational criterion, using an original differential equation formulation, is to discover the Lagrangian $L$ which when substituted into (12) will yield the original system of PDE's. This unearthing of the Lagrangian is not always a simple matter, particularly in cases of greater than second-order PDE's where higher order derivative terms appear in the Lagrangian and the Euler–Lagrange system is more complicated than in (12).

The discovery of the Lagrangian for the CAP formulation is most quickly performed by a detailed inspection process, which yields,

$$L = f_m [\nabla\psi_1 \cdot (R\epsilon_r \nabla\psi_1 + m\hat{\phi} \times \nabla\psi_2) + \nabla\psi_2 \cdot (R\mu_r \nabla\psi_2 - m\hat{\phi} \times \nabla\psi_1)] - (\epsilon_r \psi_1^2 + \mu_r \psi_2^2)/R. \tag{13}$$

This result, which is unique to within an arbitrary constant multiplier and independent additive function, may be verified by direct substitution into (12).

The second approach to establishing a variational principle is via a "stationary theorem" applicable to formally self-adjoint operators [8]. This stationary theorem is directly extendable to the matrix operator equation of (8). In particular, because of the self-adjoint nature of $\bar{A}$, if we have a boundary value problem of the type,

$$A\Psi = \Phi \tag{14a}$$

with homogeneous Dirichlet BC's

$$\Psi(R, Z, m)\,|_C = 0 \tag{14b}$$

where $\Phi(R, Z, m)$ is some known driving vector, then a functional that is stationary about the correct solution of (14) is given by

$$G = 2\langle \Psi, \Phi \rangle - \langle \Psi, A\Psi \rangle \tag{15}$$

where the inner products are defined in (10).

The conversion of the CAP system in (8) to one of the form in (14) is accomplished by the simple change of variables,

$$\Psi(R, Z, m) = \psi(R, Z, m) - \beta(R, Z) \tag{16a}$$

$$\Phi(R, Z, m) = -A\beta(R, Z) \tag{16b}$$

where $\beta(R, Z)$ is any arbitrary vector function satisfying the same boundary conditions on $C$ as does $\psi(R, Z, m)$. Substituting (16) into (15) yields

$$G = -\langle \psi, A\psi \rangle - \langle \psi, A\beta \rangle + \langle \beta, A\psi \rangle + \langle \beta, A\beta \rangle. \tag{17}$$

Using direct vector calculus operations on the combination of the second and third inner products, which is commonly referred to as the bilinear concomitant of $\psi$ and $\beta$, it will be found that $G$ can be written as

$$\begin{aligned} G = \{ &-\langle \psi, A\psi \rangle + \oint_C \psi_1 f_m (R\epsilon_r \nabla\psi_1 + m\hat{\phi} \times \nabla\psi_2) \\ &+ \psi_2 f_m (R\mu_r \nabla\psi_2 - m\hat{\phi} \times \nabla\psi_1) \cdot \hat{n}\, |dc|\} \\ &- \left\{ -\langle \beta, A\beta \rangle + \oint_C \beta_1 f_m (R\epsilon_r \nabla\beta_1 + m\hat{\phi} \times \nabla\beta_2) \right. \\ &\left. + \beta_2 f_m (R\mu_r \nabla\beta_2 - m\hat{\phi} \times \nabla\beta_1) \cdot \hat{n}\, |dc| \right\}. \end{aligned} \tag{18}$$

This can be recast into a more compact form by noting that the terms within each set of curly brackets can be recombined to yield a surface integral of the exact form of the Euler–Lagrange functional in (11) and (13). The result is

$$G = \int_S L(R, Z, \psi_1, \psi_2, \nabla\psi_1, \nabla\psi_2)\, dR\, dZ$$

$$- \int_S L(R, Z, \beta_1, \beta_2, \nabla\beta_1, \nabla\beta_2)\, dR\, dZ = F_\psi - F_\beta. \tag{19}$$

The stationary functionals $G$ and $F$, as given in (17) and (11), respectively, thus differ only by a functional of the arbitrary and independent vector $\beta$ and its derivatives: namely $F_\beta$, whose first variation with respect to the solution vector $\psi$ is zero. The Euler–Lagrange and stationary theorem approaches thus yield stationary functionals which are precisely equivalent in the variational sense.

In numerical applications of this variational criterion, using the finite-element method, it is often convenient to change variables and select as the fundamental unknowns the $\phi$-components of the modal fields, $e_{\phi,m}(R, Z) = \psi_1/R$ and $h_{\phi,m}(R, Z) = \psi_2/R$. If linear basis functions are used to approximate the potentials $\psi_1$ and $\psi_2$ then the last quadratic term in the Lagrangian in (8), $(\epsilon_r\psi_1^2 + \mu_r\psi_2^2)/R$, will introduce a nonintegrable infinite singularity along the $Z$ axis, where $R = 0$. The change of variables previously mentioned eliminates this singularity effect, but it then becomes necessary to know the boundary conditions obeyed by $e_{\phi,m}$ and $h_{\phi,m}$ along the section(s) of the $Z$ axis which bound the surface $S$. These boundary conditions can be obtained via a judicious cross substitution and limiting procedure using Maxwell's equations, and are given here for reference purposes:

$$e_{\phi,m}(R, Z)\,|_{R=0} = h_{\phi,m}(R, Z)\,|_{R=0} = 0, \quad \text{for } m^2 \neq 1 \tag{20a}$$

$$3\frac{\partial h_{\phi,m}}{\partial R} + \left(\frac{\partial \ln \epsilon_r}{\partial R}\right) e_{\phi,m}\,\Big|_{R=0} = 0, \quad \text{for } m^2 = 1 \tag{20b}$$

$$3\frac{\partial h_{\phi,m}}{\partial R} + \left(\frac{\partial \ln \mu_r}{\partial R}\right) h_{\phi,m}\,\Big|_{R=0} = 0, \quad \text{for } m^2 = 1. \tag{20c}$$

The homogeneous Dirichlet BC's for $m^2 \neq 1$, in (20a), appear as an obvious result of the continuity and single-valuedness of the vector EM field as the $Z$ axis is approached from all constant azimuth paths. The Cauchy BC's for the case of $m^2 = 1$, in (20b) and (20c), reduce to homogeneous Neumann BC's, (radial derivatives equal to zero), for the case of media composed of uniform material bodies of revolution.

A final important topic associated with the variational formulation concerns the physical interpretation of the stationary functional $F$, as displayed in (11) and (13). Using simple substitutions from (3), it can be shown that the Lagrangian in (13) can be written in terms of the modal vector electromagnetic field as

$$L = -R(\epsilon_r \bar{e}_m \cdot \bar{e}_m + \mu_r \bar{h}_m \cdot \bar{h}_m) - 2m\hat{\phi} \cdot (\bar{e}_m \times \bar{h}_m). \tag{21}$$

A direct vector manipulation of Maxwell's curl equations for the modal fields will show that this can be alternately written as

$$L = -jR\nabla' \cdot [(I - \hat{\phi}\hat{\phi}) \cdot (\bar{e}_m \times \bar{h}_m)] \tag{22}$$

where $I$ is the identity dyadic and $\nabla'\cdot$ is the conventional three-dimensional divergence operating on the transverse (to $\hat{\phi}$) vector components of the "pseudo" Poynting vector, $\bar{e}_m \times \bar{h}_m$. Upon substituting (22) into (13), the divergence theorem can be used to transform the surface integral of $F$ into a line integral around $C$ of the outward normal of the "pseudo" Poynting vector:

$$F = -j \oint_C (\bar{e}_m \times \bar{h}_m) \cdot \hat{n} R\, |dc|. \tag{23}$$

The term "pseudo" is used because no conjugates appear in the cross products in the integrand, as would be the case if the terms were related to time-average power. The physical significance of the stationary functional $F$ can be displayed by considering the time-varying power per unit azimuth radian of the $m$th order modal field that is radiated outward from a constant-$\phi$ planar cross section. This time-varying power density can be written as

$$\frac{\partial P(\phi, t)}{\partial \phi} = \frac{1}{2\eta_0 k_0^3} \operatorname{Re}\left\{ \oint_C (\bar{e}_m \times \bar{h}_m^*) \cdot \hat{n} R \, |dc| + \left[ \oint_C (\bar{e}_m \times \bar{h}_m) \cdot \hat{n} R \, |dc| \right] e^{j2(\omega t + m\phi)} \right\} \quad (24)$$

where the integral containing the magnetic field conjugate $\bar{h}_m^*$ represents time-average power while the term in square brackets is the stationary functional $F$. The functional $F$ is clearly associated with the difference of the time-varying and time-average radiated power densities. The exact physical interpretation of the stationarity of $F$ appears somewhat illusive and the quest for such an interpretation certainly warrants further consideration.

## V. CONCLUSION

The CAP formulation provides an important foundation for performing efficient numerical computations of solutions to the often encountered class of field problems involving axially symmetric media. Using the unimoment method, scattering and radiation problems can be handled very effectively by coupling exterior radiation field series solutions to interior region Dirichlet boundary value problems, which are solved either through finite-difference simulation of the CAP differential equation system [8], or through use of the variational finite-element technique.

In addition to the CAP formulation there have been discovered two alternate coupled scalar potential representations that utilize as potentials either the two vector components of $\hat{\phi} \times \bar{e}_m$ or the components of $\hat{\phi} \times \bar{h}_m$. There is, however, apparently no Euler-Lagrange functional for these formulations.

The authors currently have a very successful and operational numerical code which solves for EM scattering by arbitrarily shaped, and generally lossy, dielectric and magnetic bodies of revolution using the variational finite-element method. A detailed description of the implementation of this numerical method, along with extensive experimental and analytical verification, will be the topic of a forthcoming paper.

## REFERENCES


[1] J. Van Bladel, *Electromagnetic Fields.* New York: McGraw-Hill, 1964, pp. 229–250.

[2] C. T. Tai, "The electromagnetic theory of the spherical luneberg lens," *Appl. Sci. Res.*, sec. B, vol. 7, pp. 133–130, 1959.

[3] K. K. Mei, "Unimoment method of solving antenna and scattering problems," *IEEE Trans. Antennas Propagat.*, vol. AP-22, pp. 760–766, Nov. 1974.

[4] R. F. Harrington, *Time-Harmonic Electromagnetic Fields.* New York: McGraw-Hill, 1961, pp. 100–103.

[5] J. A. Stratton, *Electromagnetic Theory.* New York: McGraw-Hill, 1941, p. 422.

[6] R. E. Stovall and K. K. Mei, "Application of a unimoment technique to a biconical antenna with inhomogeneous dielectric loading," *IEEE Trans. Antennas Propagat.*, vol. AP-23, pp. 335–341.

[7] P. M. Morse and H. Feshback, *Methods of Theoretical Physics.* New York: McGraw-Hill, 1953, pp. 275–280.

[8] I. Stakgold, *Boundary Value Problems of Mathematical Physics,* Vol. 2. London: Macmillan, 1968, ch. 8.

[9] M. A. Morgan and K. K. Mei, "Numerical computation of E. M. scattering by inhomogeneous bodies of revolution," *Abstracts for the 1974 URSI Symposium on E.M. Wave Theory,* London, England, July 1974.

[10] G. Strang and G. J. Fix, *An Analysis of the Finite Element Method.* Englewood Cliffs, NJ: Prentice-Hall, 1974.

[11] S. K. Chang, M. A. Morgan, and K. K. Mei, "Coupled potential formulation for 3-D E.M. boundary value problems in inhomogeneous axially symmetric media," *Abstracts for the 1975 IEEE/AP-S Symposium,* Urbana, IL, June 1975.


# Some Extensions of Babinet's Principle in Electromagnetic Theory

THOMAS B. A. SENIOR, FELLOW, IEEE

***Abstract*—The concept of resistive and conductive sheets provides a meaningful extension of Babinet's principle to surfaces which are no longer perfect. The complementary problems are described, and the appropriate field relations derived.**

Babinet arrived at the principle, which now bears his name, by comparing the diffraction pattern of an aperture with that of a complementary disk. It was later verified for scalar waves subject to a Neumann or Dirichlet boundary condition on the screen or disk, and extended to electromagnetic waves by Booker [1] who pointed out the polarization rotation of the primary field which is necessary if the screen and disk are both perfectly conducting.

These known forms of Babinet's principle are all consequences of the symmetry of the fields radiated by planar distributions and (where appropriate) the duality of electromagnetic fields. Over the years there have been a number of attempts to extend the principle to surfaces which are not perfect, for example, by Neugebauer [2] to surfaces which are absorbing, and more recently by Lang [3] to resistive surfaces. In Lang's extension the complementary structures are a perfectly conducting screen with a resistive insert and a resistive screen with a perfectly conducting insert, but the derivation has been criticized [4] for the assumptions made concerning the normal components of the field. Nevertheless, as noted by Baum and Singaraju [5], resistive sheets and their electromagnetic duals do afford an exact extension of Babinet's principle. This fact was exploited by Senior [6] in developing some generalized forms in acoustics, and we here discuss the analogous results for electromagnetic waves.

Manuscript received May 4, 1976; revised August 22, 1976. This work was supported by the U.S. Air Force Office of Scientific Research under Grant 72-2262.

The author is with the Radiation Laboratory, University of Michigan, Ann Arbor, MI 48109.

Dialog DataStar

options | logoff | feedback | help

databases | easy search

## Advanced Search: INSPEC - 1969 to date (INZZ)

limit

Search history:

| No. | Database | Search term | Info added since | Results | |
|---|---|---|---|---|---|
| 1 | INZZ | radar ADJ cross ADJ section AND finite ADJ element ADJ analysis | unrestricted | 53 | show titles |
| 2 | INZZ | 1 AND axisymmetric | unrestricted | 1 | show titles |

hide | delete all search steps... | delete individual search steps...

Enter your search term(s): Search tips

whole document

Information added since: or: none
(YYYYMMDD)

search

Select special search terms from the following list(s):

- Classification codes A: Physics, 0-1
- Classification codes A: Physics, 2-3
- Classification codes A: Physics, 4-5
- Classification codes A: Physics, 6
- Classification codes A: Physics, 7
- Classification codes A: Physics, 8
- Classification codes A: Physics, 9
- Classification codes B: Electrical & Electronics, 0-5
- Classification codes B: Electrical & Electronics, 6-9
- Classification codes C: Computer & Control
- Classification codes D: Information Technology
- Classification codes E: Manufacturing & Production
- Treatment codes
- INSPEC sub-file
- Publication types

Language of publication

Top - News & FAQS - Dialog

*AIRCRAFT DESIGN **SOFTWARE** ANALYSIS AND APPLICATION DATA,*

*COMPUTATIONAL FLUID DYNAMIC, AERODYNAMIC, **FINITE ELEMENT ANALYSIS***

*AIRCRAFT STABILITY AND CONTROL , STATIC AND DYNAMICS, AIRCRAFT COST*

*AIRCRAFT PERFORMANCES , AIRCRAFT ENGINE & POWER PLANT*

*AEROELASTICITY , MANUFACTORY PLAN, AIRPLANE PROJECT MANAGEMENT*

*AIRCRAFT SYSTEMS ELECTRICS, HYDRAULIC, LANDING GEAR , ETC.*

***THE GREATEST COLLECTION***

***OF AERONAUTICAL & AEROSPACE***

***SOFTWARE APPLICATION AND DATA***

32 CD ROMS : ZIPPED FILES ABOUT AERONAUTICAL & AEROSPACE SUBJECTS

- EVERYTHING YOU NEED TO DESIGN AIRCRAFT & HELICOPTER
- EVERYTHING YOU NEED TO BUILD AIRCRAFT & HELICOPTER
- EVERYTHING YOU NEED TO CERTIFY AND TESTING AIRCRAFT & HELICOPTER
- EVERYTHING YOU NEED TO LEARN HOW FLY AIRCRAFT & HELICOPTER
- EVERYTHING YOU NEED TO REPAIR AIRCRAFT & HELICOPTER
- EVERYTHING YOU NEED TO MANAGER AIRCRAFT & HELICOPTER

- EVERYTHING YOU NEED TO KNOW HOW PILOT AIRCRAFT & HELICOPTER

## WHAT YOU WILL RECEIVE:

| | |
|---|---|
| 91 PROFESSIONAL AERONAUTICAL TESTED SOFTWARE PACKAGES | 963 DEMO & SHAREWARE AERONAUTICAL SOFTWARE |
| 11.5 MILLION OF INTERNET PAGES | 1200 AIRCRAFT & COPTER IMAGES |
| 900 DRAWING CAD FILES | 750 AERONAUTICAL SOURCE CODE |
| 65 AIRCRAFT MANUALS | 38 AIRCRAFT PARTS MANUALS |
| 65 AIRCRAFT OPERATION MANUAL | 365 AIRCRAFT REPORTS |
| 211 AIRCRAFT BOOKS | 52 3D AIRCRAFT CAD MODELS |
| 12 COMPLETE AIRCRAFT PROJECTS | AND MORE ..... |
| 21 GIG BYTE OF COMPRESSED FILES | 62 GIG BYTE EXPANSE FILES |

## IN DETAILS

| | | |
|---|---|---|
| COMPLETE AIRCRAFT PROJECTS | CAD Drawing | CATIA, ACAD, PRO/E, SOLID WORKS, UNIGRAPHICS, |
| | REPORTS | PS, PDF, MSWord . Powerpoint |
| | Application Worksheet | Excell, MathCAD, MatLab, etc |
| | CFD & FEM MODEL | ANSYS, NASTRAN ABAQUS, FLUENT VSAERO, PMARC |

| | |
|---|---|
| AIRCRAFT DESIGN AND ANALYISIS | Software & data |
| MECHANICAL AIRCRAFT DESIGN | Software & data |
| AERODYNAMICS & CFD | Software & data |
| AIRFLOW VISUALIZATION | Software |

| | |
|---|---|
| AIRFOIL DESIGN &ANALYSIS | Software & data |
| AIRCRAFT CFD MODELS | COMPUTATIONAL FLUID DYNAMIC MODEL OF AIRCRAFT AND SINGLE ELEMENTS |
| AIRCRAFT PERFORMANCES | Software & data |
| AIRCRAFT STABILITY & CONTROL | Software & data |
| AIRCRAFT DYNAMICS & CONTROL | Software & data |
| AIRCRAFT ENGINES DESIGN AND MAINTENANCE | Software & data |
| AIRCRAFT PROPELLERS DESIGN AND ANALYSIS | Software & data |
| AIRCRAFT LOADS | Software & data |
| AIRCRAFT MATERIALS | Software & data |
| AIRCRAFT COMPOSITE MATERIAL DESIGN AND MANUFACTORY | Software & data |
| AIRCRAFT STRUCTURE DESIGN AND MANUFACTORY | Software & data |
| AIRCRAFT FINITE ELEMENT MODELS | FEM MODEL for MSC/NASTRAN, FEMAP, ABAQUS, ANSYS NISA , COSMOS , MSC/PATRAN ABOUT AIRCRAFT PARTS HOW WINGS, FUSELAGE, AILERON, TAILS, RUDDER, ETC. |
| AEROELASTICITY | Software & data |
| AIRCRAFT SYSTEMS SIZING AND ANALYSIS | Software & data |
| AIRCRAFT ELECTRIC SYSTEM | Software & data |
| AIRCRAFT POWER PLANT | Software & data |
| AVIONIC SYSTEM | Software & data |
| AIRINC | Software & data |
| AIRCRAFT HYDRAULIC SYSTEM | Software & data |

| | |
|---|---|
| AIRCRAFT DE-ICE SYSTEM | Software & data |
| AIRCRAFT LANDING GEAR | Software & data |
| AIRCRAFT SYSTEM SIMULATION | Software & data |
| AIRCRAFT MANUFACTORY PLANS | Software & data |
| AIRCRAFT COST | Software & data |
| AIRCRAFT MARKETING | Software & data |
| AIRCRAFT FORECAST | Software & data |
| MATHCAD AERONAUTICAL APPLICATION | Works Sheet |
| MAT LAB AERONAUTICAL APPLICATION | Work Sheets |
| SOURCE CODE FOR AERONAUTICAL APPLICATION | IN FORTRAN, BASIC, QBASIC, PASCAL, C++, LABVIEW VISUAL BASIC, JAVA , CGI, VRML, |
| AERONAUTICAL DATABASE WITH EVERY AIRPLANE DATA AND SKETCH FROM 1980 TILL 2000 | MILITARY AIRCRAFT , COMMERCIAL AIRCRAFT , GENERAL AVIATION AIRCRAFT , VLM, HOMEBUILT, ULTRA-LIGHT, GLIDE WAR BIRDS ETC . |
| COMPLETE AIRWORTHINESS DIRECTIVE | FAA, FAR, JAR, CAA, ENAC-RAI, CAA-AU, etc |
| AERONAUTICAL STANDARD | MIL, AQAP NAS. DoD. SAE etc |
| AIRCRAFT MAINTENANCE MANUAL | PDF Format |
| AIRCRAFT OPERATIVE MANUAL | PDF Format |
| AIRCRAFT PART MANUFACTURE APPROVAL | PDF Format |
| AIRCRAFT PARS MANUAL | PDF Format |
| AIRCRAFT SUPPLEMENTAL CERTIFICATION | |
| AIRFRAME & POWER-PLANT | Software & data |
| MECHANICAL AERONAUTICAL | Software & data |
| DESIGNER AIRCRAFT REPRESENTATIVE | Software & data |

| | |
|---|---|
| I.A. | Software & data |
| AIRCRAFT TESTING | Data , Project and Testing procedure |
| AIRCRAFT GROUND TESTING | Data , Project and Testing procedure |
| AIRCRAFT FLIGHT TESTING | Data , Project and Testing procedure |
| WIND TUNNEL | Data , Design and Testing procedure |
| AIRCRAFT SIMULATION GAMES AND PROFESSIONAL | Software & data |
| AIRCRAFT TRAINING COURSE AND EXAMS TESTING | Software & data |
| 3D AIRCRAFT MODELS IN 3D STUDIO, MAYA, CAD, IGES, etc | Software & data |
| MORE 600 AIRCRAFTS DATA , PICTURE AND SKETCH | Every Graphics format |
| AERONAUTICAL BOOKS and REPORT | Pdf, MSWord , PS format |

***FAQ: Everything You Need and Want to Know about These Packages.***

***Question :HOW MUCH WILL THE 32 AERONAUTICAL CDS WILL COST?***

***Answer : $ 650 US Dollar***

***Question :WHAT FORM OF PAYMENT IS ACCEPTABLE?***

***Answer :*** **You will use *www.westernunion.com* (1 day) (fastest and the best way)**

***Question :CAN I ORDER THROUGH E-MAIL?***

***Answer : YES , Press here for order by e-mail :***

***Question ::HOW I WILL RECEIVE THE 32 AERONAUTICAL CD S?***

***Answer :The parcel will be sent registered with FedEx by airmail*** http://www.fedex.com/

***Question: How long before I receive the parcel?***

***Answer: Upon receipt of your order (including payment), your package will be sent by priority post to FedEx for delivery to your address. (Please check your FedEx office for delivery times from Europe to your country.)***
**http://www.fedex.com/**

***Question :How will you guarantee that the CDs will be delivered to me?***

***Answer : As professional engineers, working in the aerospace industry, our goal is to be able to continue advanced research projects .Over the years, all of this data has been collected and stored. We have been able to put it all together in CD format and make it available to you at this incredible price. Our desire and intent is to secure a steady clientele on an international basis. In order to do that we must act with the highest integrity and honor.*** **We already have so many satisfied customers through magazine advertising that we decided to expand our network. This aeronautical CD collection has unbelievable value for you!. These CDs are remarkable tools, allowing you to organize your data and software programs, which in turn allows you to improve your understanding and knowledge of any and all aeronautical issues.**

***Question Why I should pay the goods in advance ?***

***Answer : WE ARE MOVING FOR JOB REASON UP AND DOWN EUROPE AND NORTH AMERICA . WE Hve figure out that this is the best way.***

***Question About a detailed list for every single application***

***Answer :It is very hard to compile a complete list , there are to many data and software, anyway to can ask BY E-MAIL if what you need or looking for is include.***

***Please feel free to contact us regarding any question and/or orders BY E-MAIL***

***Your Question BY E-MAIL***

***Our Answer BY E-MAIL***

THE TEXT, WHICH IS LOCATED BELOW - IT IS LIKE A ONLY KEYWORDS FOR SEARCH ENGINES.

KEY WORDS

AIRCRAFT DESIGN, AIRCRAFT MANAGEMENT, AIRCRAFT SALES , AIRCRAFT IMAGES , DWG FILES CATIA FILES , UNIGRAPHIGS FILES PRO ENGINEERIN MECHANIC, SOLID WORK FILES CAD COMPUTER AID DESIGN CAE COMPUTER AID ENGINEERING FEM FINITE ELEMENT METHOD FEA **FINITE ELEME ANALYSIS** AERODYNAMICS SUBSONIC SUPERSONIC TRANSONIC ODE ORDINAL DIFFERENTIAL EQUATION PDE PARTIAL DIFFERENTIAL EQUATION CFD COMPU FLUID DYNAMIC AIRCRAFT GEOMETRY AIRFRAME SPAR WING, SPAR FLANGES, RIB, SKIN, SPAR WEB, SHEAR WEB , LONGITUDINAL STIFFENER, STRU ARRANGEMENT FOR WING, STIFFENERS, TRANSVERSE FRAMES, AIRCRAFT NOSE, CENTRAL FUSELAGE, REAR FUSELAGE, VERTICAL TAIL, RUDDER, FLAP , I MAIN PLANE O CENTRAL SECTION OUTER WING TIP, HORIZONTAL TAIL TIP ELEVATOR FUSELAGE ELEVATOR, AILERON FLAP, WINGLET COCKPIT , RIB RIVETED TO SKIN , LIGHTNESS HOLES, RIB STIFFENERS, CUT OUTS FOR STIFFENERS, WING SKIN AIRCRAFT DESIGN, AEROBATICS AIRCRAFT, AERODYNAMICS FP AEROFOIL, AFTERBURNER, AGRICULTURAL AIRCRAFT, AILERON, AIRBRAKE, AIR CONDITIONING, AIRCRAFT COST, ACQUISITION COST , DIRECT OPERATING COST, INDIRECT OPERATI AIRCRAFT PROJECT PROBLEMS, AISLE , ALUMINUM, ALLOY ANGLE OF ATTACK , AOA, APPROACH SPEED, ASPECT RATIO, MACH, ATE, ATMOSPHERIC PROPERTIES, AUTO GYRO , AUT AUXILIARY POWER UNIT AVAILABLE SEAT MILES , AVIONICS SYSTEM BITE , BLEED AIR , BOMB. BRACED WING , BRAKE , BREGUET RANGE , BUSINESS AIRCRAFT , BYPASS ENGI CAMBER CANARD , FORE PLANE , KIT PLANE, HOME BUILD RC MODELER , CARBON FIBER, CARGO, CEILING ,CENTER OF GRAVITY CENTER OF PRESSURE CHORD CIVIL AIRCRAFT CI AIRCRAFT CLIMB, COCKPIT COMMUNICATION SYSTEM COMMUTER AIRCRAFT, COMPOSITE , CONCEPTUAL DESIGN CONTAINER , CONTROL LINKAGE , CONTROL SURFACE, CONVERSION TABLE , CORROSION CANFIELD AIRCRAFT DESIGN PROJECTS , AEROBATIC AIRCRAFT , SHORT RANGE JET TRANSPORT AIRCRAFT , FORTUNATO SICURO AERONAUTICAL AEROSPACE ENGINEER , SI TRANSPORT AIRCRAFT , STOL AIRLINER , SHORT HAUL 500 SEAT AIRLINER , EXECUTIVE JET AIRCRAFT, SUPERSONIC NAVAL V STOL FIGHTER , CLOSE AIR SUPPORT STRIKE A ASTOVL , CRUISE PERFORMANCE , DECISION MAKING PROCESS DEEP STALL , DEFECT DELAY RATE , DELTA PLAN FORM , DESIGN CRUISING SPEED , DIRECTIONAL CONTROL, DOOR BUBBLE FUSELAGE , DRAG COEFFICIENT , DRAG POLAR , WING BOX, WING POSITION, WING LOADING , WING GROSS AREA , WING DESIGN , WING GEOMETRY , WING DESIGN, W AIRCRAFT , WEAPON , WEAPON BAY V STOL AIRCRAFT , UNDERCARRIAGE , TIRE , TWIST TWIN FUSELAGE, TURBOPROP ENGINE, TURBOJET ENGINE, TURBOFAN ENGINE, T TAIL , T TRAILING EDGE DEVICE, TOILET LAVATORY , TITANIUM , TILT ROTOR AIRCRAFT THRUST WEIGHT RATIO THICKNESS CHORD RATIO TEST EQUIPMENT , TAKE OFF DISTANCE, TAIL PLAN SWEEP WING SWEEPBACK WING SWEEP, SURVIVABILITY , SUPERCRITICAL AIRFOIL , STRUT , STRINGER , STALL, STEALTH , STABILITY AND CONTROL, SPOILER , FIN , SPECIF SPAN , SONIC BOOM, SHORT RANGE AIRCRAFT SECONDARY POWER SYSTEM SEAT RANGE CAPABILITY S TOVL, RUNWAY RUDDER ROTORCRAFT ROLL, ROCKET , REQUIREMENT , RELIABILIT STATIC STABILITY REGIONAL AIRCRAFT, RECONNAISSANCE AIRCRAFT , RANGE, RADAR SYSTEM, **RADAR CROSS SECTION**, PYLON , PROPULSIVE EFFICIENCY, PROPULSION, PROPELLE AIRCRAFT , PRESSURIZATION, PRESSURE CABIN PRELIMINARY DESIGN, POWER PLANT , PLASTIC PITCHING MOMENT PITCH UP , PAYLOAD, PAYLOAD RANGE DIAGRAM , PASSENGER A PARAMETRIC DESIGN, OXYGEN SYSTEMS, NOSE GEAR , NOMENCLATURE, NAVIGATION , NOISE NAVAL FIGHTER NARROW-BODY AIRCRAFT , MISSION RADIUS MISSILE, MISSILE APPROACH TRAINER AIRCRAFT, AIRCRAFT TYPE , CARGO AIRCRAFT , MICRO LIGHT AIRCRAFT MASS BALANCING MASS ESTIMATE MARKER SURVEY MANEUVER, MANEUVERABILITY , MAINTENAI MAINTAINABILITY MAIN GEAR , MAGNESIUM ALLOY, MACH NUMBER , MACH DRAG, LONG RANGE AIRCRAFT LONGITUDINAL STABILITY AND CONTROL LOAD CARRY STRUCTURE , LOAD FACT AIRCRAFT, LIFT TO DRAG RATIO LIFT CURVE SLOPE LIFT COEFFICIENT LEADING EDGE DEVICE LANDING GEAR , LAYOUT , RETRACTION, LANDING DISTANCE , LAMINAR FLOW, DRIVEN AIRCRAFT , INTERIOR DESIGN , INTAKE , INSURANCE , INCIDENCE ANGLE , ICE PROTECTION SYSTEM , HYDRAULIC SYSTEM, HORIZONTAL STABILIZER GUST LOAD ALLEVIAT GROUND ATTACK AIRCRAFT, GROSS WEIGHT, GLOBAL POSITION SYSTEM BY SATELLITE , GEOMETRIC WING CHORD , GALLEY, FUSELAGE CROSS SECTION DRAG, ECM , ECONOMY EJECT ELECTRIC POWER SYSTEM, ELEVATOR, EMERGENCY EXIT , EMPIRICAL DATABASE, ENGINE FAILURE , ENGINE LOCATION, FUSELAGE BURIED , WING MOUNTED ENVIRONMENTAL CONTROL EXHAUST , FAULT TREE ANALYSIS , FEEDER LINER , FIELD PERFORMANCE, INTERCEPTOR AIRCRAFT, FLIGHT CONTROL SYSTEM , FLUTTER , FORWARD SWEEP WING, , FUEL CONSU FURNISHING, FREIGHTER AIRCRAFT STRUCTURE BASIC ELASTICITY , STRESS, FORCE AND STRESS, EQUATION OF EQUILIBRIUM, PLANE STRESS, BOUI CONDITION, STRESS TRANSFORMATIONS, PRINCIPAL STRESS, MOHR'S CIRCLE OF STRESS, STRAIN, COMPATIBILITY EQUATIONS, PLANE STRAIN, ST

TRANSFORMATIONS PRINCIPAL STRAINS MOHR'S CIRCLE OF STRAIN STRESS-STRAIN RELATIONSHIPS EXPERIMENTAL MEASUREMENT OF SURFACE STRAINS DIMENSIONAL PROBLEMS IN ELASTICITY, STRESS FUNCTIONS, St VENANT'S PRINCIPLE, DISPLACEMENTS BENDING OF AN END LOADED CANTILEVER , TO SOLID SECTIONS, PRANDT STRESS FUNCTION SOLUTION, ST. VENAT WARPING FUNCTION SOLUTION THE MEMBRANE ANALOGY TORSION OF A NARROW RECT STRIP, ENERGY METHODS OF STRUCTURAL ANALYSIS STRAIN ENERGY AND COMPLEMENTARY ENERGY, TOTAL POTENTIAL ENERGY, PRINCIPAL OF VIRTUAL W PRINCIPLE OF THE STATIONARY VALUE OF THE TOTAL POTENTIAL ENERGY, THE PRINCIPLE OF STATIONARY VALUE OF THE TOTAL COMPLEMENTARY ENE APPLICATION TO DEFLECTION PROBLEMS APPLICATION TO THE SOLUTION OF STATICALLY INDETERMINATE SYSTEMS, UNIT LOAD METHOD, PRINCIPLE SUPERPOSITION THE RECIPROCAL THEOREM TEMPERATURE EFFECTS, BENDING OF THIN PLATES PURE BENDING OF THIN PLATES, PLATES SUBJECT TO BEN TWISTING, PLATE SUBJECT TO A DISTRIBUTE TRANSVERSE LOAD, COMBINED BENDING AND IN-PLATE LOADING OF A THIN RECTANGULAR PLATE, BENDING PLATES HAVING A SMALL INITIAL CURVATURE, ENERGY METHOD FOR THE BENDING OF THIN PLATES , STRUCTURAL INSTABILITY, EULER BUCKLING OF INELASTIC BUCKLING, EFFECT OF INITIAL IMPERFECTIONS, STABILITY OF BEAMS UNDER TRANSVERSE AND AXIAL LOADS, ENERGY METHOD FOR THE CALCU BUCKLING LOADS IN COLUMNS, BUCKLING OF THIN PLATES INELASTIC BUCKLING OF PLATES EXPERIMENTAL DETERMINATION OF CRITICAL LOAD FOR A F LOCAL INSTABILITY, INSTABILITY OF STIFFENED PANELS FAILURE STRESS IN PLATES AND STIFFENED PANELS TORSION INSTABILITY OF THIN WALLED TENSION FIELD BEAMS, ANALYSIS OF AIRCRAFT STRUCTURES , PRINCIPLES OF STRESSED SKIN CONSTRUCTION, LOADS ON STRUCTURAL COMPONENTS, FUN STRUCTURAL COMPONENTS FABRICATION OF STRUCTURAL COMPONENTS , STRUCTURAL IDEALIZATION, BENDING , SHEAR AND TORSION OF OPEN AND CLOS WALLED TUBES , GENERAL ENGINEER'S THEORY OF BENDING FOR OPEN AND CLOSED TUBES, GENERAL STRESS, STRAIN AND DISPLACEMENT RELATIONSHIPS AND SINGLE CELL CLOSED TUBES, SHEAR OF OPEN TUBES SHEAR OF CLOSED TUBES, TORSION OF CLOSED TUBES, TORSION OF OPEN TUBES EFFECT OF BOO ANALYSIS OF OPEN AND CLOSED TUBES, DEFLECTION OF OPEN AND CLOSED TUBES , MULTICELL TUBES, BENDING , TORSION, SHEAR, VARIATION OF MODULUS, SHEAR CENTER AND FLEXURAL AXIS, EFFECTS OF TAPER , DEFLECTION OF MULTI CELL TUBES, LIMITATION OF THE ANALYSIS , AXIAL CONS SHEAR STRESS DISTRIBUTION AT BUILT IN END, AXIAL CONSTRAINT STRESSES IN A DOUBLY SYMMETRICAL SINGLE CELL, FOUR BOOM TUBE TORSION, DIFFUSION, AXIAL CONSTRAINT STRESSES IN A DOUBLY SYMMETRICAL, SINGLE CELL, SIX BOOM TUBE SUBJECTED TO SHEAR, AXIAL CONSTRAINT STRESSE TUBES, MATRIX METHODS OF STRUCTURAL ANALYSIS, STIFFNESS MATRIX FOR AN ELASTIC SPRING, STIFFNESS MATRIX FOR TWO ELASTIC SPRINGS IN LIN ANALYSIS OF PIN JOINTED FRAMEWORKS APPLICATION TO STATICALLY INDETERMINATE FRAMEWORKS, MATRIX ANALYSIS OF SPACE FRAMES, STIFFNESS MAT UNIFORM BEAM, FINITE ELEMENT METHOD FOR CONTINUUM STRUCTURES , AIRWORTHINESS, FACTORY OF SAFETY, FLIGHT ENVELOPE, LOAD FACTOR DETER SYMMETRIC MAN OEUVRE LOADS, NORMAL ACCELERATIONS ASSOCIATED WITH VARIOUS TYPES OF MANEUVERS, GUST LOAD ELEMENTARY AEROELATICITY , DISTRIBUTION AND DIVERGENCE, CONTROL EFFECTIVENESS AND REVERSAL, STRUCTURAL VIBRATION , DYNAMIC AERO ELASTIC PHENOMENA AERO-ELASTI FLUTTER COMPOSITE MATERIAL ,ELASTIC AXLE, ADHESIVES, BEAM THEORY, BENDING, CANTILEVER PANEL, PANELS IN LATTICE, BEAMS, SOLID AIRFOI FORCES IN LATTICE, BLEEDER , SECONDARY BOND, EFFECT OF SHAPE, BUSHING & ATTACHMENTS, CANTILEVER PANEL, COMPOSITE AS TWO PHASE MATE ENVIRONMENTAL EFFECTS, CORE MATERIALS , FOAMS, HONEYCOMB, POLYSTYRENE, POLYURETHANE, PVC FOAM, ROHACELL, WOOD , CORNER FLOX, CUTTIN DUCTILITY, WICKING, FABRICS, TOW, TRIAX, UNIDIRECTIONAL, FAILURE MODES, FATIGUE , IN COMPOSITE, IN METAL , FEMALE MOLDS , ADDING JO LAYING UP, SPLASH MOLD , MAKING AN OPEN LAY-UP , MAKING JOGGLE OFFSETS , PERMANENT TOOLING , QUICK & EASY , VACUUM BAGGING , FILLERS MICRO , MILLED GLASS , FINISHING , DRY MICRO, DISPERSED , MICRO , PURE , REX TAYLOR , SMUDGE STICK , SURFACE , WARMING LAYER, SANDIN FLEXIBILITY IN DESIGN , HOT WIRE FOAM CUTTING, ATOMIC BONDS FRACTURE MECHANICS, BRITTLE FRACTURE, BUCKLING , CRACK STOPPING, GRIFFIT GLASS IN TWO PHASE MATERIALS PLASTIC FLOW GRIFFITH, HOLLOW STRUCTURES , LOCAL STIFFENING, SANDWICH SKIN WING, HOOK'S LAW , HOR WIRE SQUARING TOOL, PROCEDURE, HYBRID DEIGNS , JOINING, BONDING FOAM BLOCKS, PREPREG STRIPS, JOINING STRUCTURES, ADHESIVE JOINTS, BUSH ATTACHMENTS , COMPOSITE STRUCTURE, KIT MANUFACTURES METHODS, KNITTED FIBERS , TRIAX, DOUBLE BIAS, ADVANCED COMPOSITE AILERON PROGRAM , L ACOUSTIC ULTRASONIC, ADVANCED COMPOSITE STRUCTURE TECHNOLOGY PROGRAM , NASA, VERTICAL FIN, ADVANCE COMPOSITES ENGINEERING, ADVANCE COMPOSITE REPAIR GUIDE, AE AERO ELASTIC TAILORING, AEROLITE, AERO RESEARCH, AERO RESEARCH LABORATORIES , MELBOURNE, AEROSPATIALE , AUGUSTA SPA, AIRBUS INDUSTRIES, AIRCRAFT RESEARCH ASS AIRWORTHINESS , AQAP 24 , MIL9858, ASSEMBLY GUIDANCE SYSTEMS, ATS SMOKE EMISSION REQUIREMENTS AUTOMATION AVCO CORPORATION, BAAKELAND, BAKELITE, BELL LCAV VEHICLE, BERP BRITISH EXPERIMENTAL ROTOR, BOEING AIRPLANE COMPANY , BRAKES , REPAIR, COMPUTER BASED ANALYSIS PRO MC DONNELL DOUGLAS , BRISTOL CARBONDEK, BRISTOL COMPOSITE MATERIALS ENGINEERING LTD , BRITISH AEROSPACE PLC BRITISH AIRWAYS, BVID, VISIBLE IMPACT DAMAGE, CAA, CIVIL AVIATION AUTHORITY, CASA, CVD CHEMICAL VAPOR DEPOSITION, CHOPPED STRAND MAT, CIBA GEIGY PLASTIC, CN PROFILING MACHINE, COMPOSITE AUTOMATION ENGINEERING INC. COMPOSITE TRANSPORT WING DEVELOPMENT PROGRAM, CONTINUOUS STRAND MAT, DESIGN TECHNOLOGIES LTD, DOWTY DUNLOP LTD, EATF EXTERNAL APPLIED THERMAL FIELS , ELSVIER APPLIED SCIENCE PUBLISHERS, EMI RFI SHIELDING, ELECTRO MAGNETIC INTERFACE, ENGINEERING DESIGN AUTHOR FEDERAL AVIATION ADMINISTRATION, ADVISOR CIRCULAR, COMPOSITE AIRCRAFT STRUCTURES FIBERITE EUROPE, FILAMENT WINDING, DOUBLE HEADED MACHINE, GLASS IMPREGNATION B NON LINEAR WINDING, PLASTER MATURING TWIN-BED, POLAR WINDER, FISHER, FOD, FOREIGN OBJECT DAMAGE, FORMICA, FREQUENCY ANALYSIS, GALVANIC CORROSION, GENERAL ELE , GE, GERBER CORPORATION, GLASS TRACER, GRIFFITH, HAIL DAMAGE, HANDLE PAGE VICTOR CONSTANT SPEED UNIT DRIVE, HELICOPTER ROTOR BLADES, BERP, BRITISH EXPERIM PROGRAMMER, WESTLAND AUGUSTA, LYNX, SEA KING, HOLOGRAPHIC INTERFEROMETER, HOLOGRAPHY, ULTRASONIC, HOVERCRAFT, INSTITUTION OF MECHANICAL ENGINEERS IMPACT DAMAG CAMERA, JET PROBE SCANNING, LIGHTNING STRIKE AND PROTECTION, LUFTHANSA, MECHANICAL IMPEDANCE TESTING, MESSERCHMITT BOLKOW BLOOM , GMBH, MILAN PROJECTILE LAU MASSACHUSETTS INSTITUTE OF TECHNOLOGY, MOD, MINISTRY OF DEFERNCE, STANDARD NACA , NATIONAL ADVISORY COMMITTEE FOR AERONAUTICS, NASA NATIONAL AERONAUTICS AN ADMINISTRATION, AIRCRAFT ENERGY EFFICIENCY PROGRAM, NATIONAL ENGINEERING LABORATORY, NATO, NORTH ATLANTIC TREATY ORGANIZATION, NBC, NUCLEAR BIOLOGICAL CHEMIC NAVAL ORDINANCE LABORATORY, PHILLIPS , PRATT & WHITNEY, PREPEG CUTTING LASER, RECIPROCATING KNIFE, ROUTER, ULTRASONIC KNIFE, WATER JET, PROPELLER BLADES DE HYDROMANTIC, HAMILTON STANDARD, SIX-BLADE, PROP-FAN PROFULSION, PROP FAN BLADES FATIGUE TESTING, FLEXURAL TEST RIG, LIGHTNING STRIKE TEST RING, PRVT, PRO READINESS VERIFICATION TESTING, PURSLOW, QUALITY CONTROL, RADIOGRAPHY, RAE, ROYAL AEROSPACE ESTABLISHMENT, TECHNICAL REPORTS RAM, RADAR ABSORBENT MATERIAL RC **CROSS SECTION**, REDUX BONDING, RESIN INJECTION MOLDING, RILEY, ROCKET MOTOR NOZZLES, ROLLS ROYCE ENGINE, ROYAL AIR FORCE CENTRAL SERVING DEVELOPMENT ESTABLISH SOCIETY, RULE OF MIXTURES SERVICE ENGINEERED MODIFICATION, SGTF, STRESS GENERATED THERMAL FIELD, SPECKLE PHOTOGRAPHY, SPECTROSCOPY, STEALTH, STRUCTURAL TESTING TAPE LAYING MACHINE, TAPE WINDING THERMAL DAMAGE, AGING, THERMOGRAPH, THERMOPLASTIC INJECTION MOLDING, TOOL RITE, TORNADO ENGINEERING AUTHORITY, TRANSDUCER, P DRY COUPLED, ULTRASONIC ATTENUATION, FLAW DETECTION, GONIOMETRY, HOLOGRAPHY, RESONANCE, SPECTROSCOPY, VELOCITY MEASUREMENT, UNIVERSITY OF DELFT AERODYNAMIC DI UNIVERSITY OF LEEDS, LOUGHBOROUGH, USAF, UNITED STATE AIR FORCE, U.S. MARINE CORPS, USN, UNITED STATES NAVY UV ULTRA VIOLET WESTLAND AERO STRUCTURES LTD PER TAKE OFF DISTANCE, LANDING DISTANCE , POWER LOADING, WING LOADING TURBINE ENGINE, AIRCRAFT ENGINE RECIPROCATING ENGINE, AIRCRAFT PERFORMANCE, COCKPIT CONTROLS, ENGINE INSTRUMENTS, STARTING, RUN UP, TAKEOFF AND CLIMB, CRUISE OPERATION , MIXTURE MANAGEMENT, DE APPROACH, & SHUTDOWN, EMERGENCIES, ENGINE NOMENCLATURE, SCREW, FILLISTER HEAD, WASHER, LOCK, PLAIN, COVER, VALVE ROCKER, GASKET, HE SHAFT, SCREW DRIVE, BUSHING, PUSH ROD, SPRING, HOUSING, PACKING, NUT, FLANGED, CYLINDER ASSEMBLY, O-RING, RETAINER, ROTOR COIL ASS EXHAUST VALVE, RETAINER, INTAKE VALVE, SPRING, OUTER, INNER, INTAKE VALVE GUIDE VALVE, INSERT SPARK PLUG, INTAKE FLANGE, PIN AND ASSEMBLY, PISTON, RING COMPRESSION, OIL CONTROL RINGER, SCRAPER, LIFTER ASSEMBLY, HYDRAULIC VALVE, RETAINING , LYCOMING, CONTINE CRANKCASE, CRANKSHAFT, CRANKSHAFT DAMPERS, CONNECTING RODS, PISTON RINGS, CAMSHAFT, TAPPETS, VALVES, TURBOCHARGERS , STARTER ADAPTER, SWITCH, BOOST PUMP, FUEL SELECTOR, MIXTURE CONTROL, THROTTLE, PRIMER, PROP PITCH, CARBURETOR HEAT, COWL FLAPS, TACHOMETER, MANIFOLD OIL PRESSURE, TEMPERATURE, CYLINDER HEAD TEMPERATURE, EXHAUST GAS TEMPERATURE, TURBINE INLET TEMPERATURE, COMPRESSOR DISCHARGE, , GOVERNOR CONTROL LEVEL, POWER CHARTS, IAS, CHT, A/F RATIO, AIR TO FUEL RATIO, AGL, ABOVE GROUND LEVEL, ANGLE VALVE HEAD , AUSTEN AUTOMATIC CONTROLLER, BABBITT, BHP, BRAKE HORSEPOWER, BIFILAR PENDULUM DAMPER, BMP, BRAKE MEAN EFFECTIVE PRESSURE, BOOST, BOOST BOOTSTRAPPING, BORE SCOPE, BORDEN TUBE, BOWDEN CABLE, BREATHER, BTC, BEFORE TOP CENTER , BTU, BRITISH THERMAL UNIT, BUTTERFLY VALV COMPETITION FOR AIRCRAFT FLYING EFFICIENCY, CHOKE, CHT , CYLINDER HEAD TEMPERATURE, COMPRESSION RATIO, CREEP, CRITICAL ALTITUDE, PRESSURE, DETONATION, DISPLACEMENT, DYNAMIC COUNTERWEIGHTS, EGT, EXHAUST GAS TEMPERATURE, FLOAT CARBURETOR , FLOW DIVIDER, , FOUR CYCLE, FWF, FIREWALL FORWARD, GALLERY, OIL PASSAGEWAY IN CRANKCASE, HELI COIL, IAS, INDICATED AIRSPEED , INCONEL, INDUCTION SYSTEM ANIFOLD , INTERCOOLER , MANIFOLD PRESSURE, MANIFOLD VALVE , MP , NIMONIC, NI REST , NITRALLOY NORMALLY ASPIRATED, NORMALIZE, NAT TRANSPORTATION SAFETY BOARD, NTSB, OAT, OUTSIDE AIR TEMPERATURE, OTTO CYCLE, OVER BOOST, P LEAD , MAGNETO PRIMARY LEAD WIRE, PMA, MANUFACTURE APPROVAL, PREIGNITION, PRESSURE RATIO, PSI , POUND PER SQUARE INCH. , RANKINE, REID VAPOR PRESSURE , SAE, SOCIETY OF AU ENGINEERS , SFC , SPECIFIC FUEL CONSUMPTION, STC, SUPPLEMENTAL TYPE CERTIFICATE , STOICHIOMETRIC , SUPERCHARGER, TBO, TIME BETWEEN O THROTTLE BUTTERFLY, TIT, TURBINE INLET TEMPERATURE, TURBOCHARGER, UPPER DECK, VENTURI, VENIER, VOLUMETRIC EFFICIENCY A, AEROBATIC S OIL SYSTEM, G, GEAR REDUCTION PROP DRIVE, H HELICOPTER MODEL, HORIZONTAL ORIENTATION, I, FUEL INJECTED, L, LEFT-HAND ENGINE ROTATI OPPOSED CYLINDER CYLINDERS, S, SUPERCHARGED LYCOMING T, TURBOCHARGED, TS TURBO SUPERCHARGED CONTINENTAL, V, VERTICAL ORIENTATION ST CONTROL DYNAMIC STABILITY & CONTROL AIRCRAFT SYSTEMS PRINCIPLES OF ELECTRICITY,, STATIC ELECTRICITY, ELECTROMOTIVE FORCE, CURRE RESISTANCE, POWER, BASIC ELECTRICAL SYSTEM (DC), PRINCIPLES OF MAGNETISM, ELECTROMAGNETISM, STORAGE BATTERIES, CIRCUIT PROTECTION, CAUSE OF ELECTRICAL CIRCUIT FAILURE, ALTERNATING CURRENT, GENERATING DIRECT CURRENT, GENERATING ALTERNATING CURRENT, MISCELLANEOUS E COMPONENTS, ELECTRICAL SYSTEMS, GENERATORS (DC), ALTERNATORS, COMBINED AC/DC ELECTRICAL SYSTEMS, ALTERNATORS ,MAINTENANCE, MOTORS MOTORS ( AC), MANUFACTURER DOCUMENTATION, TURBINE ENGINES , TURBINE ENGINE HISTORY, FACTORS AFFECTING THRUST, AIRCRAFT JET ENGINES, ENGINE COMPONENTS, TURBINE ENGINE IGNITION SYSTEMS, TURBINES, MAIN BEARINGS, EXHAUST SECTION, THRUST REVERSES, ENGINE NOISE, ACC SECTION, ENGINE STARTING SYSTEMS, WATER INJECTION , REQUIRED MAINTENANCE , MANUFACTURE DOCUMENTATION, LUBRICATION AND COOLING SYSTE SUMP SYSTEM, DRY-SUMP SYSTEM, TYPICAL DRY-SUMP SYSTEMS, COOLING SYSTEMS, MANUFACTORY DOCUMENTATION AIRCRAFT PROPELLERS, PROPELLER CONSTANT SPEED PROPELLER, PROPELLER SYSTEM OPERATION, SYNCHROPHASERS, PREFLIGHT AND MAINTENANCE, HYDRAULIC AND PNEUMATIC SYSTEMS , H FLUID, HYDRAULIC SYSTEM COMPONENTS, HYDRAULIC PUMPS , ACCUMULATORS, FLUID LINE AND FITTING, FILTERS, ACTUATING CYLINDERS, PNEUMATIC FUEL SYSTEMS , TURBINE ENGINE FUELS, FUEL SYSTEM CONTAMINATION, MINIMIZING CONTAMINATION, FUEL HANDLING SAFETY, FUEL SYSTEM THEORY, CONTROLS, FUEL SYSTEM COMPONENTS, FUEL SYSTEM MAINTENANCE, ENVIRONMENTAL SYSTEMS, NEED FOR OXYGEN ATMOSPHERE'S COMPOSITION, ATMOSP PRESSURE, TEMPERATURE AND ALTITUDE, PRESSURIZATION, AIR-CONDITIONING AND PRESSURIZATION SYSTEMS, AIR DISTRIBUTION, HEATING SYST SUPPLEMENTAL OXYGEN SYSTEMS , LANDING GEAR SYSTEMS, SHOCK STRUTS, MAIN LANDING GEAR, EMERGENCY EXTENSION AND SAFETY SYSTEMS, NOSE BRAKE SYSTEMS, WHEELS AND TIRES, MANUFACTURE DOCUMENTATION, FIRE PROTECTION SYSTEMS, PORTABLE EXTINGUISHERS, ZONE CLASSIFICATIONS ,

SYSTEMS, DETECTORS,, OVERHEAT WARMING, EXTINGUISHER SYSTEMS, AERODYNAMIC CONTROL AND PROTECTION SYSTEMS, TABS, HIGH LIFT DEVICES, E LAYER CONTROL DEVICES, VORTEX GENERATORS, FLIGHT CONTROL SYSTEMS, PROTECTION AIRCRAFT OEM , AIRCRAFT MAINTENANCE MANUFACTURE BOEING BOMBARDIER, CESSNA, PIPER, BRITISH AEROSPACE AEROSPATIALE BRITISH AEROSPACE CONCORDE, PUMA, AIRBUS, BA, BRITISH AEROSPACE PLC EAP, EXPERIMENTAL A PROGRAMME , HARRIER, HAWEK, BAE SEA HARRIER BEECH STARSHIP BELL-BOEING V22 OSPREY TILT ROTOR AIRCRAFT B707, B727 B 737, B 747, B767 , B7 B777 B CHINOOK , CAN ADAIR CHALLENGER, DASSAUL MIRAGE DE HAVILLAND AIRCRAFT DH91 ALBATROSS CANADA DASH 8, DH 98 MOSQUITO DH 103 HORN EFA, EUROPEAN FIGHTER AIRCRAFT FOKKER AIRCRAFT CORPN , F 50, F 100 , GENERAL DYNAMICS CORP. F 16 , F 111 , GRUMMAN, A6 INTRUDER POV GOSSAMER CONDOR, HANDLEY PAGE, HEMPEN, VICTOR, HAWKER SIDDELY AVIATION, KESTREL P1127 LEAR FAN LOCKHEED, C5A GALAXY, C130 HERCULES L STAR, MCDONNELL DOUGLAS A4 SKY HAWK F15 AV-8B GR5 MD/NORTHROP PANAVIA TORNADO, PARTENAVIA , VILCANAIR , TECAM, PIPER CHEYENNE ROCKW SEPCAT JAGUAR VICKERS VC10 WESTLAND AUGUSTA EH101 HELICOPTER SEA KING , W 30/300 X WING VTOL AIRCRAFT, SIKORSKY

# Titles

To view one or many selected titles scroll down the list and click the corresponding boxes. Then click display at the t page. To view one particular document click the link above the title to display immediately.

Documents 1 to 4 of 4 from your search **"(finite ADJ element ADJ analysis AND aircraft) AND radar ADJ cross ADJ section"** in all the available information:
Number of titles selected from other pages: 0

☐ **Select All**

☐ 1 display full document

*2002.* (INZZ) Computation of **radar cross section** of jet engine inlets with a nonuniform **cross section** and complex internal structures.

☐ 2 display full document

*1999.* (INZZ) An efficient algorithm for the RCS modulation prediction from jet inlet-engines.

☐ 3 display full document

*1998.* (INZZ) A numerical scheme combining FEM, MoM and modal techniques for large inlet scattering.

☐ 4 display full document

*1997.* (INZZ) CEM for **radar cross section** application.

| Selection | Display Format | Display in | ERA SM Electronic Redistribution & Archivir |
|---|---|---|---|
| ◉ from this page<br>○ from all pages | ◉ Full<br>○ Free<br>○ Short<br>○ Medium<br>○ Custom<br>Help with Formats | ◉ HTML<br>○ Tagged (for tables) | Copies you will redistribute: ☐<br>Employees who will access archived record (s): ☐<br>Help with ERA |

**Sort your entire search result by** Publication year Ascending

Top - News & FAQS - Dialog

| | Type | L # | Hits | Search Text | DBs | Time Stamp |
|---|---|---|---|---|---|---|
| 1 | BRS | L1 | 0 | (radar adj cross adj section) same (FEM) | USPAT | 2004/08/27 09:00 |
| 2 | BRS | L2 | 0 | (radar adj cross adj section) same (finite adj element adj model) | USPAT | 2004/08/27 08:59 |
| 3 | BRS | L3 | 0 | (radar adj cross adj section) same (finite adj element adj analysis) | USPAT | 2004/08/27 09:00 |
| 4 | BRS | L4 | 16 | (radar adj cross adj section) same (calculate) | USPAT | 2004/08/27 09:00 |
| 5 | BRS | L5 | 0 | (radar adj cross adj section) same (axi-periodic) | USPAT | 2004/08/27 09:00 |
| 6 | BRS | L6 | 0 | (radar adj cross adj section) and (axi-periodic) | USPAT | 2004/08/27 09:00 |
| 7 | BRS | L7 | 0 | (axi-periodic) | USPAT | 2004/08/27 09:00 |
| 8 | BRS | L8 | 21 | (radar adj cross adj section) same simulation | USPAT | 2004/08/27 09:01 |
| 9 | BRS | L9 | 0 | ((radar adj cross adj section) same simulation) and (finite adj element adj method) | USPAT | 2004/08/27 09:01 |
| 10 | BRS | L10 | 0 | ((radar adj cross adj section) same simulation) and (FEM) | USPAT | 2004/08/27 09:02 |
| 11 | BRS | L11 | 36 | ((radar adj cross adj section)).ti. | USPAT | 2004/08/27 09:02 |
| 12 | BRS | L12 | 3 | ((radar adj cross adj section)).ti. and engines | USPAT | 2004/08/27 09:04 |
| 13 | BRS | L13 | 51 | (jet adj engine) and modeling and (cross adj section) | USPAT | 2004/08/27 09:04 |
| 14 | BRS | L14 | 1 | (jet adj engine) and modeling and (cross adj section) and radar | USPAT | 2004/08/27 09:04 |

Table of Contents

Previous chapter

# Jets-In-Crossflow Mixing

*Clifford E. Smith, Principal Investigator*
*Co-investigators: Daniel B. Bain and James D. Holdeman*
*CFD Research Corporation/NASA Lewis Research Center*

## Research Objective

The objectives of this work were to identify improved mixing schemes for rich-burn/quick-mix/lean-burn combustors applicable to advanced aircraft engines and to assess the effects of design parameters on mixing effectiveness. Efforts were focused on jet mixing in rectangular cross-sectional geometries.

## Approach

Numerical parametric studies were performed on different orifice configurations. The computational analyses were performed using a three-dimensional Navier-Stokes flow solver (CFD-ACE) capable of analyzing turbulent reacting flows in complex geometries. The numerical results were examined using an interactive visualization package (CFD-VIEW).

## Accomplishment Description

Over 60 orifice configurations were analyzed and assessed. The modeled geometry consisted of a rectangular duct with a row of jets on the top and bottom walls. Isothermal flow conditions were assumed. Systematic, parametric analyses were performed, consisting of variations in (1) orifice lateral alignment (in-line and staggered), (2) jet-to-mainstream (J) momentum flux ratio (16, 36, 64), (3) orifice aspect ratio (4:1, 2:1, 1:1, circle), (4) jet-to-mainstream mass flow (MR) ratio (2.0, 0.50, 0.25), and (5) orifice spacing-to-duct height (S/H) ratio ($0.125 <= S/H <= 1.5$). The numerical calculations were performed with grids varying in size from 50,000-150,000 cells that required approximately 2-4 Cray Y-MP hours and 10-15 megawords of memory.

## Significance

At optimum S/H, in-line lateral arrangements produced faster initial mixing than non-impinging, staggered arrangements due to their smaller geometric orifice size. Previous publications show that S/H ((root) J) is a practical design parameter for mixing optimization even at high MR, and increasing J improves initial mixing at optimum S/H.

## Future Plans

The effect of mass flow ratio and aspect ratio on mixing effectiveness will be assessed, and emission characteristics will be inferred from existing cold-flow data.

# Publication

Bain, D. B.; Smith, C. E.; and Holdeman, J. D.: CFD Mixing Analysis of Axially Opposed Rows of Jets Injected Into Confined Crossflow. AIAA Paper 93-2044, June 1993.

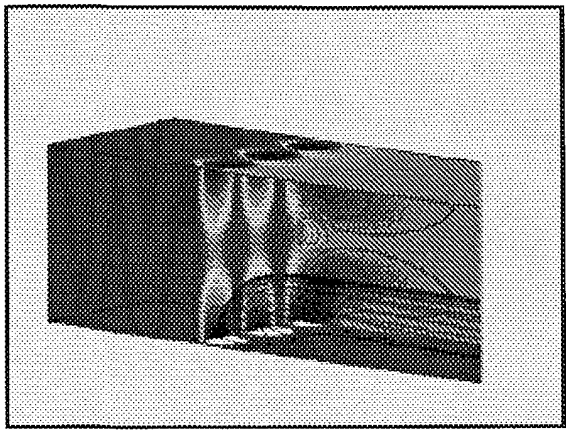

Typical jet mixing numerical results. In-line circular orifices: S/H = 0.375, J = 36, MR = 2.0. Jet mass fraction: red = 0.0 to blue = 1.0.

**Next chapter**

**Index**

*Web Work: chucas@nas.nasa.gov*

Web Images Groups News Froogle more »

"radar cross section" + "axis symmetric" + " Search Advanced Search Preferences

**Web** Results **1** - **1** of **1** for "**radar cross section**" + "**axis symmetric**" + "**finite element analysis**". (**0.22** seco

Tip: Try removing quotes from your search to get more results.

[PDF] PIERS 2004 Progress In Electromagnetic Research Symposium
File Format: PDF/Adobe Acrobat - View as HTML
... GmbH, Germany); E. Klink, R. Frech (IBM, Germany) 18:20 Time Domain Numerical Simulation Method Based on EFIE and MFIE for **Axis-Symmetric** Structure Objects H ...
sun8.dsea.unipi.it/piers04_v3/ GLANCE_DETAILED/detailed_program9.pdf - Similar pages



"radar cross section" + "axis sym Search

Search within results | Language Tools | Search Tips | Dissatisfied? Help us improve

Google Home - Advertising Programs - Business Solutions - About Google